Phytochemistry 127 (2016) 50–62

Contents lists available at ScienceDirect

Phytochemistry

journal homepage: www.elsevier.com/locate/phytochem

Phenylethanoid glycosides and phenolic glycosides from stem bark of *Magnolia officinalis*

Zhenzhen Xue, Renyi Yan, Bin Yang *

Institute of Chinese Materia Medica, China Academy of Chinese Medical Sciences, Beijing 100700, PR China

ARTICLE INFO

Article history:
Received 24 June 2015
Received in revised form 16 March 2016
Accepted 21 March 2016
Available online 13 April 2016

Keywords:
Magnolia officinalis
Magnoliaceae
Phenylethanoid glycoside
Phenolic glycoside
α-Glucosidase inhibitory effect
Cytotoxicity

ABSTRACT

An investigation of the hydrophilic constituents of the stem bark of *Magnolia officinalis* was performed and which led to isolation and identification of twenty-one previously unreported glycosides. These included eleven phenylethanoid glycosides, magnolosides F–P, and ten phenolic glycosides, magnolosides Q–Z, along with eight known compounds. Their structures were elucidated on the basis of extensive spectroscopic analyses and chemical hydrolysis methods, as well as by comparison with literature data. Most of the phenylethanoid glycosides contained an allopyranose moiety, which is rare in the plant kingdom. Magnolosides I and K as well as 2-(3,4-dihydroxyphenyl) ethanol 1-*O*-[4-*O*-caffeoyl-2-*O*-α-L-rhamnopyranosyl-3-*O*-α-L-rhamnopyranosyl-6-*O*-β-D-glucopyranosyl]-β-D-glucopyranoside showed more potent α-glucosidase inhibitory effects (IC_{50} values of 0.13, 0.27, and 0.29 mM, respectively) than the positive control, acarbose (IC_{50} value of 1.09 mM) *in vitro*. Magnolosides H, E and D also showed moderate cytotoxicity against MGC-803 and HepG2 cells with IC_{50} values of 13.59–17.16 μM and 29.53–32.46 μM, respectively.

1. Introduction

Magnolia officinalis Rehd. et Wils. is a member of the Magnoliaceae family. The stem bark of *M. officinalis* is known as Houpo in Chinese. In traditional Chinese medicine (TCM), it has been prescribed along with other TCMs for the treatment of abdominal distention and pains, dyspepsia, and asthmatic cough (Chinese Drug Dictionary, 1977). Pharmacological studies indicated that it also had anti-spasmodic (Yu et al., 2012), anti-cancer (Syu et al., 2004; Chen and Wang, 2005) and antidiabetic activities (Liu, 2009). Much research has focused on liposoluble constituents of Houpo, such as lignans, neolignans, alkaloids and sesquiterpenes (Sarker et al., 2002; Youn et al., 2007; Shen et al., 2009; Guo et al., 2011), while no systematic work on hydrophilic constituents has been performed. In previous work, two new phenylethanoid glycosides (Yu et al., 2012), one new phenolic glycoside (Yan et al., 2014) and magnolosides A-B (Yu et al., 2012) were reported, which indicated the existence of glycosides in *M. officinalis*. Of these, Magnolosides A-C were first reported in *Magnolia obovata* Thunb in 1988 (Hasegawa et al., 1988a,b). Yulanosides A-B, 2′-rhamnoechinacoside and three known phenylethanoid glycosides were also reported in tepals of *Magnolia salicifolia* (Porter et al., 2015).

Traditionally, Houpo is processed prior to clinical practice. In previous work, some water-soluble compounds were described that changed after the Houpo was processed (Yu et al., 2010). Meanwhile, Houpo is clinically used as an aqueous decoction and there may be some water-soluble components related to the pharmacological activity. Subsequently, in an attempt to search for more bioactive substances from aqueous portion of *M. officinalis*, and to clarify its material foundation of efficacy, a systematic phytochemical study was performed, which resulted in characterization of eleven new phenylethanoid glycosides (**1**–**11**), ten new phenolic glycosides (**12**–**21**) and eight known compounds (**22**–**29**) (Fig. 1). Because the anti-spasmodic activities of phenylethanoid glycosides have been performed in a previous study (Yu et al., 2012), the α-glucosidase inhibitory effects and cytotoxic activities of the isolated aqueous compounds were presented herein.

2. Results and discussion

2.1. Structural analysis

The water-soluble portion of the 70% ethanol extract of the stem bark of *M. officinalis* was subjected to sequential column

* Corresponding author.
E-mail address: ybinmm@126.com (B. Yang).

http://dx.doi.org/10.1016/j.phytochem.2016.03.011
0031-9422/

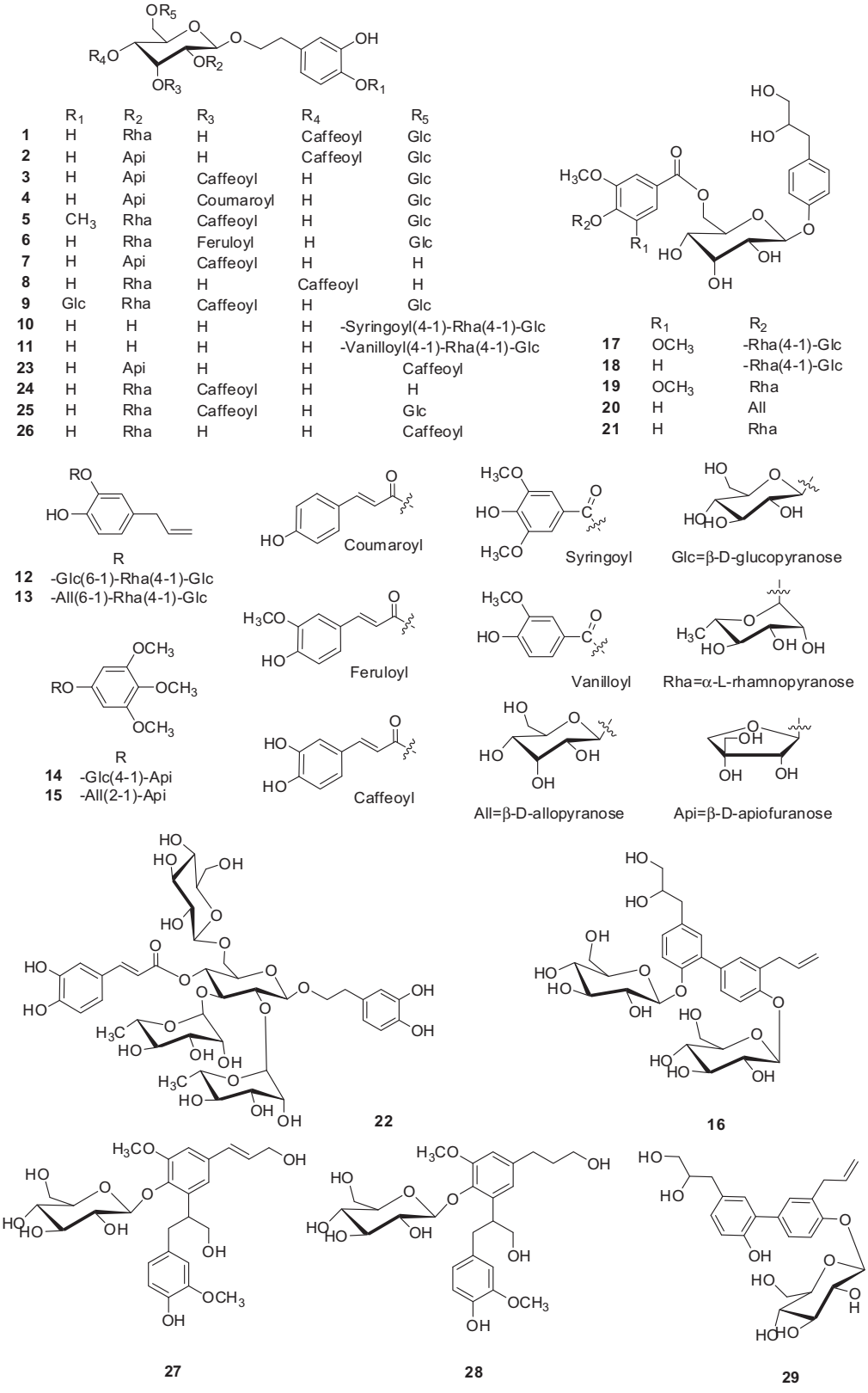

Fig. 1. Structures of **1**–**29**.

chromatography over D101 macroporous resin, MCI CHP-20P, C-18, and Sephadex LH-20, with purification using preparative HPLC to yield twenty-one novel glycosides, magnolosides F-Z (**1**–**21**). In addition, eight known ones, 2-(3,4-dihydroxyphenyl) ethanol 1-*O*-[4-*O*-caffeoyl-2-*O*-α-*L*-rhamnopyranosyl-3-*O*-α-*L*-rhamnopyranosyl-6-*O*-β-*D*-glucopyranosyl]-β-*D*-glucopyranoside (**22**) (Iwasaki and Zhou, 2013; Porter et al., 2015), magnoloside E (**23**) (Yu et al., 2012), magnoloside A (**24**) (Hasegawa et al., 1988a),

magnoloside B (Hasegawa et al., 1988b) (**25**), magnoloside D (**26**) (Yu et al., 2012), icarisides E_3 (**27**) (Toshio et al., 1988), icariside E_5 (**28**) (Miyase et al., 1989), and 1,1′-dibenzene-6′,8′,9′-trihydroxy-3-allyl-4-*O*-*β*-D-glucopyranoside (**29**) (Deng et al., 2002) were obtained as amorphous solids, and whose ^{1}H, ^{13}C NMR and MS data were consistent with those reported in the literature.

Magnoloside F (**1**) was obtained as a pale yellow amorphous powder, and its molecular formula was assigned to be $C_{35}H_{46}O_{20}$ based on HRESIMS data at *m*/*z* 785.2496 $[M-H]^-$ (calcd for $C_{35}H_{45}O_{20}$, 785.2504). The UV spectrum showed absorption maxima at 288 and 330 nm, which were assignable to a caffeoyl group. Its IR spectrum displayed absorption bands of hydroxyl (3407 cm^{-1}), conjugated carbonyl (1693 and 1630 cm^{-1}) and aromatic (1603 cm^{-1}) groups. The ^{1}H NMR spectrum of **1** exhibited characteristic signals belonging to (*E*)-caffeoyl and 3,4-dihydroxyphenylethanol moieties: two sets of ABX-type aromatic signals at δ_H 7.29 (1H, d, *J* = 1.2 Hz, H-2), 7.20 (1H, overlap, H-5), 6.79 (1H, dd, *J* = 7.8, 1.2 Hz, H-6), and δ_H 7.52 (1H, d, *J* = 1.2 Hz, H-2‴′), 7.20 (1H, overlap, H-5‴′), and 7.09 (1H, dd, *J* = 8.4, 1.2 Hz, H-6‴′); two *trans*-olefinic protons at δ_H 7.96 (1H, d, *J* = 15.6 Hz, H-7‴′) and 6.55 (1H, d, *J* = 15.6 Hz, H-8‴′), and a *β*-methylene at δ_H 3.04 (2H, t, *J* = 7.2 Hz, H-*β*) (Table 1). Additionally, three anomeric proton resonances appeared at δ_H 5.45 (1H, d, *J* = 7.8 Hz, H-1′), 4.96 (1H, d, *J* = 7.8 Hz, H-1″), and 5.66 (1H, brs, H-1‴) which correlated, respectively, with signals at δ_C 100.3, 105.6, and 97.7 in the HSQC spectrum. The methyl signal at δ_H 1.68 (3H, d, *J* = 6.0 Hz, H-6‴) and δ_C 17.9 indicated the existence of a rhamnose moiety. A series of signals in the ^{1}H NMR spectrum at δ_H 5.45 (1H, d, *J* = 7.8 Hz, H-1′), 4.18 (1H, dd, *J* = 7.8, 2.4 Hz, H-2′), 5.18 (1H, t, *J* = 2.4 Hz, H-3′), 5.50 (1H, dd, *J* = 9.6, 2.4 Hz, H-4′), 4.84 (1H, ddd, *J* = 9.6, 5.4, 1.8 Hz, H-5′), 4.57 (1H, overlap, H-6a′) and 4.10 (1H, dd, *J* = 11.4, 5.4, H-6b′) indicated a rare *β*-allopyranosyl unit in the structure of **1**. This was confirmed by comparing its NMR features with those of magnolosides A (Hasegawa et al., 1988a), B (Hasegawa et al., 1988b), C (Hasegawa et al., 1988b), D (Yu et al., 2012), and E (Yu et al., 2012) which all contained an allopyranose moiety. Another series of signals in the ^{1}H NMR spectrum at δ_H 4.96 (1H, d, *J* = 7.8 Hz, H-1″), 4.05 (1H, dd, *J* = 8.4, 7.8 Hz, H-2″), 4.23 (1H, dd, *J* = 9.6, 8.4 Hz, H-3″), 4.26 (1H, dd, *J* = 9.6, 9.0 Hz, H-4″), 3.92 (1H, m, H-5″), 4.51 (1H, dd, *J* = 11.4, 1.8 Hz, H-6a″), and 4.37 (1H, overlap, H-6b″) indicated the existence of a *β*-glucopyranosyl moiety. Further confirmation was achieved by analysis of its hydrolyzed products, in which D-allose, L-rhamnose, and D-glucose were detected by GC. The ^{1}H and ^{13}C NMR spectroscopic data of **1** were very similar to those of magnoloside B (Hasegawa et al., 1988b), except for signals being associated with the linkage of an allose moiety and its neighbor groups. An unambiguous determination of the sequence and linkage sites were obtained from the HMBC

Table 1
^{1}H NMR spectroscopic data of compounds **1**–**6** and **10**–**11** (600 MHz, pyridine-d_5).

Position	**1** δ_H (*J* in Hz)	**2** δ_H (*J* in Hz)	**3** δ_H (*J* in Hz)	**4** δ_H (*J* in Hz)	**5** δ_H (*J* in Hz)	**6** δ_H (*J* in Hz)	**10** δ_H (*J* in Hz)	**11** δ_H (*J* in Hz)
2	7.29 d (1.2)	7.26 d (1.8)	7.28 brs	7.28 d (1.8)	7.24 overlap	7.30 d (1.8)	7.19 d (1.8)	7.21 overlap
5	7.20 overlap	7.19 d (8.4)	7.19 overlap	7.19 d (7.8)	6.94 d (7.8)	7.20 overlap	7.15 d (7.8)	7.16 d (7.8)
6	6.79 dd (7.8, 1.2)	6.80 dd (8.4, 1.8)	6.84 d (7.2)	6.84 dd (7.8, 1.8)	6.86 d (7.8)	6.82 dd (7.8, 1.8)	6.75 dd (7.8, 1.8)	6.77 brd (7.8)
β	3.04 t (7.2)	3.06 t (7.8)	3.11m	3.12m	3.07 t (7.2)	3.06 t (7.2)	3.01m	3.01m
α	4.38 m	4.35 overlap	4.38 overlap	4.38 m	4.40 overlap	4.38 overlap	4.38 m	4.39 overlap
	3.81 dt (9.6, 7.8)	3.84 dt (8.4, 7.8)	3.84 dt (7.8, 7.2)	3.86 dt (9.0, 7.2)	3.81 dt (7.2)	3.78 overlap	3.93 dt (9.0, 6.6)	3.94 dt (8.4, 7.8)
All-1′	5.45 d (7.8)	5.44 d (7.8)	5.22 d (7.8)	5.25 d (7.8)	5.24 d (8.4)	5.24 d (7.8)	5.39 d (7.8)	5.39 d (7.8)
2′	4.18 dd (7.8, 2.4)	4.15 dd (7.8, 2.4)	4.19 brd (7.8)	4.19 dd (7.8, 3.0)	4.22 dd (7.8, 2.4)	4.58 overlap	4.05 dd (7.8, 3.0)	4.06 d (7.8)
3′	5.18 t (2.4)	5.17 t (2.4)	6.36 brs	6.38 t (3.0)	6.35 t (2.4)	6.38 t (3.0)	4.78 t (3.0)	4.79 brs
4′	5.50 dd (9.6, 2.4)	5.43 dd (10.2, 2.4)	4.39 overlap	4.25 overlap	4.43 overlap	4.51 overlap	4.15 dd (9.0, 3.0)	4.19 brd (7.2)
5′	4.84 ddd (9.6, 5.4, 1.8)	4.87 ddd (10.2, 5.4, 1.8)	4.51 overlap	4.54 overlap	4.52m	4.50 overlap	4.69 ddd (9.0, 6.6, 1.8)	4.67m
6′	4.57 overlap	4.55 dd (11.4, 1.8)	4.77 d (10.8)	4.79 brd (10.2)	4.76 brd (10.8)	4.76 overlap	5.31 overlap	5.24 d (11.4)
	4.10 dd (11.4, 5.4)	4.08 dd (11.4, 5.4)	4.32 overlap	4.33 overlap	4.34 brd (10.8)	4.35 overlap	4.91 overlap	4.97 dd (11.4, 6.0)
Glc-1″	4.96 d (7.8)	4.95 d (7.8)	5.07 d (7.8)	5.08 d (7.8)	5.09 d (7.8)	5.08 d (7.8)	5.31 d (7.8)	5.28 d (7.2)
2″	4.05 dd (8.4, 7.8)	4.05 t (8.4)	4.09 t (7.8)	4.10 t (8.4)	4.09 t (7.8)	4.08 t (8.4)	4.16 dd (9.0, 7.8)	4.12 t (7.2)
3″	4.23 dd (9.6, 8.4)	4.22 t (8.4)	4.26 overlap	4.27 overlap	4.28 overlap	4.26 overlap	4.24 t (9.0)	4.23 overlap
4″	4.26 dd (9.6, 9.0)	4.25 t (9.0)	4.28 overlap	4.28 overlap	4.39 overlap	4.41 overlap	4.30 t (9.0)	4.28 overlap
5″	3.92m	3.91m	3.93m	3.93m	3.94m	3.93m	3.84 ddd (9.0, 4.8, 3.0)	3.81m
6″	4.51 dd (11.4, 1.8)	4.50 dd (11.4, 1.8)	4.51 overlap	4.53 overlap	4.53 overlap	4.51 overlap	4.48 dd (11.4, 3.0)	4.44 d (10.8)
	4.37 overlap	4.36 overlap	4.40 overlap	4.40 overlap	4.41 overlap	4.40 overlap	4.40 dd (11.4, 4.8)	4.37 overlap
Rha/Api-1‴	5.66 brs	5.88 brs	5.95 s	5.96 s	5.75 s	5.77 s	6.07 d (1.2)	6.08 s
2‴	4.56 overlap	4.73 brs	4.60 overlap	4.62 overlap	4.29 overlap	4.57 overlap	4.94m	4.76 brs
3‴	4.67 dd (9.6, 3.0)				4.53 overlap	4.58 overlap	4.95m	4.83 dd (9.0, 1.8)
4‴	4.32 t (9.6)	4.64 d (9.6)	4.59 overlap	4.60 d (9.6)	4.33 overlap	4.33 overlap	4.51 t (9.0)	4.49 t (9.0)
		4.35 overlap	4.34 overlap	4.34 s				
5‴	4.77m	4.28 s	4.39 d (8.4)	4.40 overlap	4.76 overlap	4.76 overlap	4.90m	4.27 overlap
			4.25 overlap					
				4.27 overlap				
6‴	1.68 d (6.0)				1.69 d (6.0)	1.66 d (6.0)	1.70 d (6.6)	1.62 d (6.0)
2‴′	7.52 d (1.2)	7.53 s	7.53 s	7.53 d (8.4)	7.52 s	7.29 d (1.2)	7.50 s	7.80 d (1.8)
3‴′				7.17 d (8.4)				
5‴′	7.20 overlap	7.20 overlap	7.20 overlap	7.17 d (8.4)	7.22 overlap	7.20 overlap		7.41 d (8.4)
6‴′	7.09 dd (8.4, 1.2)	7.10 dd (7.8, 1.8)	7.10 d (7.2)	7.53 d (8.4)	7.07 d (7.2)	7.14 dd (7.8, 1.2)	7.50 s	7.89 dd (8.4, 1.8)
7‴′	7.96 d (15.6)	7.95 d (16.2)	7.95 d (16.2)	7.94 d (16.2)	7.92 d (15.6)	7.93 d (15.6)		
8‴′	6.55 d (15.6)	6.54 d (16.2)	6.71 d (16.2)	6.71 d (16.2)	6.68 d (15.6)	6.77 d (15.6)		
OCH_3					3.71s	3.79s	3.56s	3.63s

correlations. Correlations of H-1′ (δ_H 5.45, allose)/C-α (δ_C 71.6, phenylethanol), H-4′ (δ_H 5.50, allose)/C-9‴′ (δ_C 166.7, caffeoyl), H-1‴ (δ_H 5.66, rhamnose)/C-2′ (δ_C 73.9, allose), and H-1″ (δ_H 4.96, glucose)/C-6′ (δ_C 69.4, allose) were observed (Fig. 2). Therefore, structure **1** was established as 2-(3,4-dihydroxyphenyl)-ethyl 1-*O*-[4-*O*-caffeoyl-2-*O*-α-L-rhamnopyranosyl-6-*O*-β-D-glucopyranosyl]-β-D-allopyranoside.

Magnolosides G (**2**) and H (**3**) were isolated as pale yellow amorphous powders, sharing the same molecular formula $C_{34}H_{44}O_{20}$ based on HRESIMS *m/z* 771.2328 $[M-H]^-$ (calcd for $C_{34}H_{43}O_{20}$, 771.2348) and 771.2334 $[M-H]^-$ (calcd for $C_{34}H_{43}O_{20}$, 771.2348), respectively. Compared to the ^{1}H NMR data of **1**, there were two sets of ABX-type aromatic signals, two *trans*-olefinic protons and β-methylene signals, which indicated the existence of (*E*)-caffeoyl and 3,4-dihydroxyphenylethanol moieties in **2** and **3** (Table 1). The ^{1}H NMR spectra of **2** and **3** also indicated the existence of three sugar moieties: δ_H 5.44 (1H, d, *J* = 7.8 Hz, H-1′), 4.95 (1H, d, *J* = 7.8 Hz, H-1″), 5.88 (1H, brs, H-1‴) and δ_H 5.22 (1H, d, *J* = 7.8 Hz, H-1′), 5.07 (1H, d, *J* = 7.8 Hz, H-1″), 5.95 (1H, s, H-1‴), respectively; however, there were no typical methyl signals for a rhamnose moiety. In the ^{1}H NMR spectrum of 2, characteristic signals of an apiose moiety were observed, including an anomeric proton at δ_H 5.88 (1H, brs, H-1‴) coupled with a vicinal proton at δ_H 4.73 (1H, brs, H-2‴), ABq signals at δ_H 4.64 (1H, d, *J* = 9.6 Hz, H-4a‴) and 4.35 (1H, overlap, H-4b‴), as well as a methylene at δ_H 4.28 (2H, s, H-5‴). Meanwhile, in the ^{13}C NMR spectrum (Table 2), the signals assigned to apiose at δ_C 106.6 (d), 77.9 (d), 80.8 (s), 75.7 (t), and 66.2 (t) were consistent with reported data (Yu et al., 2012). Hydrolysis of **2** resulted in liberation of D-allose, D-apiose and D-glucose. Finally, all connectivities within **2** were established by an HMBC experiment: correlations of H-1′ (δ_H 5.44, allose)/α-C (δ_C 71.3, phenylethanol), H-4′ (δ_H 5.43, allose)/C-9‴′ (δ_C 166.7, caffeoyl), H-6′ (δ_H 4.55, 4.08, allose)/C-1″ (δ_C 105.6, glucose), and H-1‴ (δ_H 5.88, apiose)/C-2′ (δ_C 74.0, allose) were observed. Thus, **2** was assigned as 2-(3,4-dihydroxyphenyl)-ethyl 1-*O*-[4-*O*-caffeoyl-2-*O*-β-D-apiofuranosyl-6-*O*-β-D-glucopyranosyl]-β-D-allopyranoside. Marked differences between **2** and **3** were in the carbon chemical shifts of allose, and the correlation of H-3′ (δ_H 6.36, allose)/C-9‴′ (δ_C 167.5, caffeoyl) suggested that the caffeoyl moiety was connected with C-3′ of allose. Thus, **3** was elucidated as 2-(3,4-dihydroxyphenyl)-ethyl 1-*O*-[3-*O*-caffeoyl-2-*O*-β-D-apiofuranosyl-6-*O*-β-D-glucopyranosyl]-β-D-allopyranoside.

Magnoloside I (**4**) was isolated as a pale yellow amorphous powder, and its molecular formula was $C_{34}H_{44}O_{19}$ based on

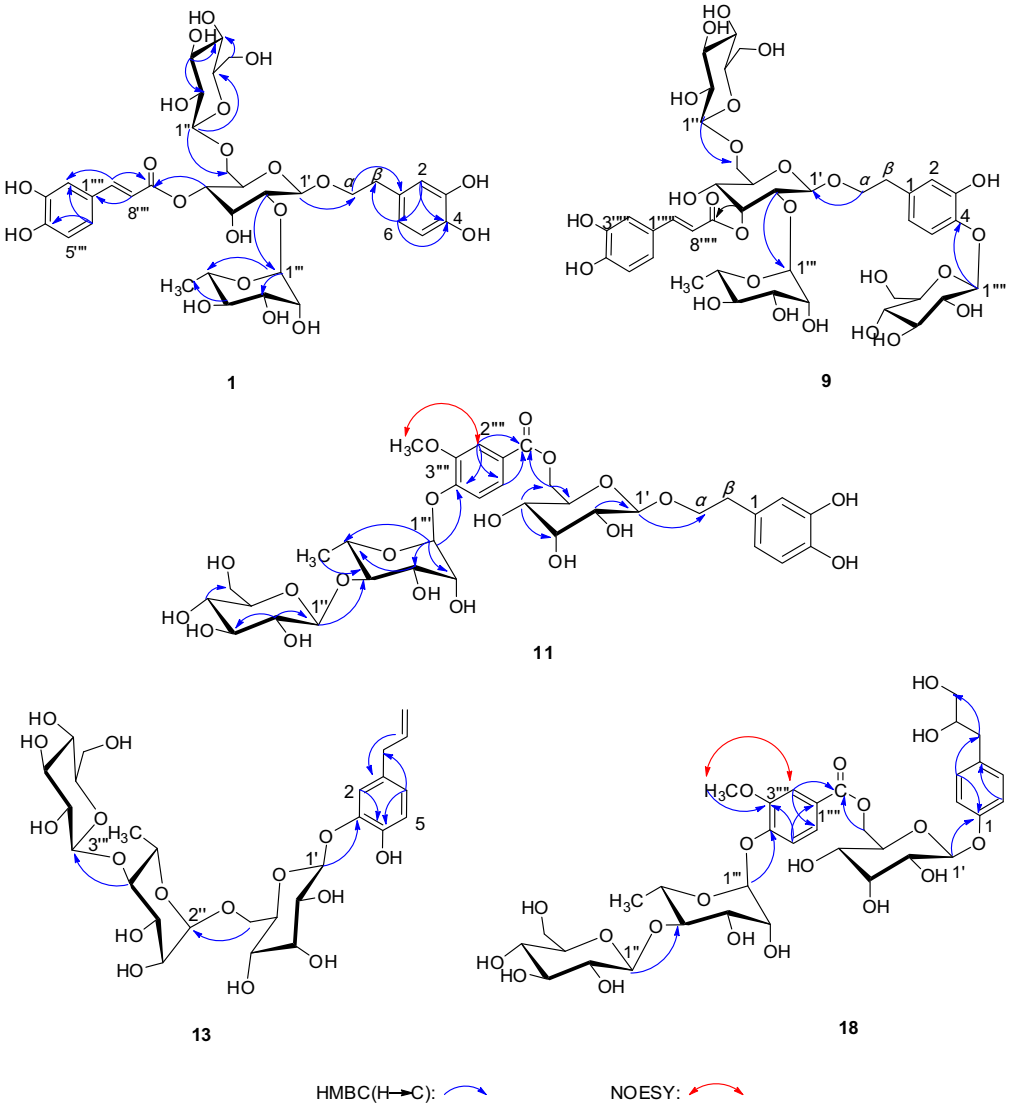

Fig. 2. Key HMBC and NOESY correlations of **1**, **9**, **11**, **13**, and **18**.

Table 2
^{13}C NMR spectroscopic data of compounds **1**–**6** and **10**–**11** (150 MHz, pyridine-d_5).

Position	**1** δ_C	**2** δ_C	**3** δ_C	**4** δ_C	**5** δ_C	**6** δ_C	**10** δ_C	**11** δ_C
1	130.7	130.6	130.5	130.5	132.5	130.7	130.5	130.5
2	117.7	117.6	117.6	117.6	117.6	117.7	117.5	117.5
3	147.7	147.0	147.0	147.1	147.9	146.9	147.2	147.2
4	145.6	145.6	145.5	145.6	147.2	145.6	145.6	145.6
5	116.7	116.5	116.5	116.6	112.8	116.6	116.5	116.5
6	120.7	120.7	120.7	120.6	120.3	120.8	120.4	120.5
β	36.4	36.3	36.4	36.4	36.4	36.5	36.4	36.4
α	71.6	71.3	71.3	71.4	71.4	71.6	71.5	71.43
All-1′	100.3	100.3	100.5	100.5	100.6	100.6	102.3	102.4
2′	73.9	74.0	72.1	72.0	72.5	72.1	72.5	72.4
3′	65.5	65.9	70.6	70.7	70.5	70.5	73.0	73.0
4′	70.7	70.8	66.5	66.6	66.5	66.4	69.7	69.4
5′	71.9	72.0	75.1	75.2	75.1	75.1	73.1	73.1
6′	69.4	69.5	69.8	69.8	69.7	69.6	66.2	65.8
Glc-1″	105.6	105.6	105.7	105.7	105.7	105.8	106.9	106.7
2″	75.2	75.2	75.2	75.3	75.2	75.2	76.5	76.3
3″	78.3	78.3	78.3	78.4	78.3	78.3	78.5	78.5
4″	71.5	71.5	71.5	71.6	71.5	71.7	71.4	71.3
5″	78.5	78.5	78.5	78.6	78.5	78.5	78.6	78.6
6″	62.7	62.7	62.6	62.7	62.6	62.6	62.6	62.6
Rha/Api-1‴	97.7	106.6	106.3	106.4	98.1	98.0	103.3	100.4
2‴	72.4	77.9	77.6	77.7	72.0	72.4	71.6	71.41
3‴	72.7	80.8	80.7	80.8	72.4	72.6	72.3	72.3
4‴	74.1	75.7	75.9	75.9	74.0	74.1	84.8	84.4
5‴	69.8	66.2	66.5	66.7	69.8	69.7	69.5	69.3
6‴	18.7				18.7	18.7	18.4	18.4
1⁗	126.8	126.8	126.9	126.1	126.9	126.5	126.6	125.1
2⁗	115.9	115.9	115.9	130.8	116.0	111.3	107.4	113.7
3⁗	146.9	147.7	147.5	116.8	147.5	148.9	153.7	150.2
4⁗	150.6	150.6	150.2	161.4	150.2	151.1	139.4	150.3
5⁗	116.6	116.7	116.6	116.8	116.6	116.6	153.7	116.7
6⁗	122.2	122.2	122.2	130.8	122.2	124.0	107.4	123.8
7⁗	146.5	146.4	146.0	145.3	146.0	145.7	166.3	166.5
8⁗	114.6	114.6	115.4	115.5	115.3	115.6		
9⁗	166.7	166.7	167.5	167.4	167.5	167.5		
OCH_3					56.0	55.9	55.9	55.8

HRESIMS data at *m/z* 755.2377 $[M-H]^-$ (calcd for $C_{34}H_{43}O_{19}$, 755.2399). In the ^{1}H NMR spectrum of **4**, typical *trans*-olefinic protons at δ_H 7.94 (1H, d, J = 16.2 Hz, H-7⁗) and 6.71 (1H, d, J = 16.2 Hz, H-8⁗), as well as AA′BB′-type aromatic protons at δ_H 7.53 (2H, d, J = 8.4 Hz, H-2⁗, 6⁗) and 7.17 (2H, d, J = 8.4 Hz, H-3⁗, 5⁗) were observed (Table 1). Additionally, three anomeric proton resonances appeared at δ_H 5.25 (1H, d, J = 7.8 Hz, H-1′), 5.08 (1H, d, J = 7.8 Hz, H-1″), and 5.96 (1H, s, H-1‴). Comparison of the ^{1}H NMR data of **4** with those of **3** indicated that the caffeoyl moiety in **3** was replaced by a *trans*-*p*-coumaroyl group in **4**. The HMBC spectrum of **4** had key long-range correlations: H-1′ (δ_H 5.25, allose)/α-C (δ_C 71.4, phenylethanol), H-3′ (δ_H 6.38, allose)/C-9⁗ (δ_C 167.4, coumaroyl), H-2′ (δ_H 4.19, allose)/C-1‴ (δ_C 106.4, apiose), H-1″ (δ_H 5.08, glucose)/C-6′ (δ_C 69.8, allose). Thus, structure **4** was elucidated as 2-(3,4-dihydroxyphenyl)-ethyl 1-*O*-[3-*O*-coumaroyl-2-*O*-*β*-*D*-apiofuranosyl-6-*O*-*β*-*D*-glucopyranosyl]-*β*-*D*-allopyranoside.

Magnolosides J (**5**) and K (**6**) were isolated as pale yellow amorphous powders, having the same molecular formula of $C_{36}H_{48}O_{20}$ based on HRESIMS *m/z* 799.2651 $[M-H]^-$ (calcd for $C_{36}H_{47}O_{20}$, 799.2661) and 799.2650 $[M-H]^-$ (calcd for $C_{36}H_{47}O_{20}$, 799.2661), respectively. There were also two sets of ABX-type aromatic signals, two *trans*-olefinic protons and a *β*-methylene group detected in the ^{1}H NMR spectra of **5** and **6** (Table 1), indicating the existence of (*E*)-caffeoyl and 3,4-dihydroxyphenylethanol moieties. Additionally, a methoxyl group signal appeared at δ_H 3.71 (3H, s) in **5** and 3.79 (3H, s) in **6**, and three anomeric proton resonances were observed at δ_H 5.24 (1H, d, J = 8.4 Hz, H-1′), 5.09 (1H, d, J = 7.8 Hz, H-1″), 5.75 (1H, s, H-1‴) in **5** and δ_H 5.24 (1H, d, J = 7.8 Hz, H-1′), 5.08 (1H, d, J = 7.8 Hz, H-1″), 5.77 (1H, s, H-1‴) in **6**, respectively. The methyl signal at δ_H 1.69 (3H, d, J = 6.0 Hz) in **5** and δ_H 1.66 (3H, d, J = 6.0 Hz) in **6** indicated the existence of a rhamnose group. Comparison of the NMR data of **5** with those of **1** suggested one hydroxyl in a phenylethanol moiety in **1** being replaced by a methoxyl group in **5**. In the HMBC spectrum, cross-peaks were observed between the protons of methoxyl (δ_H 3.71) and C-4 (δ_C 147.2), H-6 (δ_H 6.86) and C-4 (δ_C 147.2), which showed that the methoxyl was linked to C-4. Therefore, **5** was assigned as 2-(3-hydroxy-4-methoxyphenyl)-ethyl 1-*O*-[3-*O*-caffeoyl-2-*O*-α-*L*-rhamnopyranosyl-6-*O*-*β*-*D*-glucopyranosyl]-*β*-*D*-allopyranoside.

Compared to the NMR spectra of **5**, the differences in those of **6** suggested that the caffeoyl moiety in **5** was replaced by a *trans*-feruloyl group in **6**, *i.e.*, the methoxyl was linked to C-3⁗ of a caffeoyl group. This assumption was confirmed by an HMBC correlation between δ_H 3.79 (3H, s) and C-3⁗ (δ_C 148.9). Further evidence was obtained by comparing the NMR data of **6** with those of cistanoside J (Nan et al., 2013). So **6** was deduced to be 2-(3,4-dihydroxyphenyl)-ethyl 1-*O*-[3-*O*-feruloyl-2-*O*-α-*L*-rhamnopyranosyl-6-*O*-*β*-*D*-glucopyranosyl]-*β*-*D*-allopyranoside.

Magnolosides L (**7**) and M (**8**), respectively, were assigned the molecular formulae of $C_{28}H_{34}O_{15}$ and $C_{29}H_{36}O_{15}$ deduced from HRESIMS *m/z* 609.1817 $[M-H]^-$ (calcd for $C_{28}H_{33}O_{15}$, 609.1819) and 623.1979 $[M-H]^-$ (calcd for $C_{29}H_{35}O_{15}$, 623.1976), respectively. The ^{1}H NMR data of **7** (Table 3) also indicated there were two sets of ABX-type aromatic signals: δ_H 7.26 (1H, brs), 7.20 (1H, d, J = 7.8 Hz), 6.81 (1H, brd, J = 7.8 Hz) and δ_H 7.54 (1H, brs), 7.21 (1H, overlap), 7.10 (1H, brd, J = 8.4 Hz); two *trans*-olefinic protons δ_H 7.98 (1H, d, J = 15.6 Hz) and 6.73 (1H, d, J = 15.6 Hz); *β*-methylene δ_H 3.12 (2H, m) and two anomeric protons δ_H 5.31 (1H, d, J = 7.8 Hz, H-1′) and 6.06 (1H, brs), respectively. Comparison with the NMR data of **2** and **7**, indicated that in the latter there

Table 3
^{1}H (600 MHz) and ^{13}C NMR (150 MHz) spectroscopic data of compounds **7** and **8** in pyridine-d_5.

Position	**7**		**8**	
	δ_C	δ_H (J in Hz)	δ_C	δ_H (J in Hz)
1	130.3		130.7	
2	117.4	7.26 brs	117.7	7.27 d (1.8)
3	146.9		147.7	
4	145.4		145.6	
5	116.3	7.20 d (7.8)	116.7	7.23 overlap
6	120.4	6.81 brd (7.8)	120.7	6.77 dd (8.4, 1.8)
β	36.2	3.12m	36.5	3.06 t (7.8)
α	71.1	4.33 overlap	71.6	4.33m
		3.90m		3.86 dt (9.6, 6.6)
All-1′	100.4	5.31 d (7.8)	100.4	5.53 d (7.8)
2′	72.2	4.33 overlap	74.0	4.70 dd (7.8, 3.0)
3′	70.7	6.50 brs	65.7	5.25 t (3.0)
4′	66.7	4.45 overlap	70.6	5.62 dd (10.2, 3.0)
5′	76.4	4.45 overlap	73.5	4.74 ddd (10.2, 4.8, 1.8)
6′	62.2	4.49 overlap	62.0	4.30 overlap
		4.36 overlap		4.18 dd (12.0, 4.8)
Rha/Api-1″	106.3	6.06 brs	97.7	5.72 brs
2″	77.4	4.66 brs	72.5	4.61 brs
3″	80.6		72.7	4.31 overlap
4″	75.7	4.32 overlap	74.1	4.28 overlap
5″	66.4	4.39 overlap	69.8	4.80m
		4.28 d (11.4)		
6″			18.7	1.67 d (6.6)
1‴	126.7		126.8	
2‴	115.8	7.54 brs	115.9	7.54s
3‴	147.4		147.0	
4‴	150.2		150.6	
5‴	116.4	7.21 overlap	116.6	7.23 overlap
6‴	121.9	7.10 brd (8.4)	122.2	7.10 dd (7.8, 1.8)
7‴	145.7	7.98 d (15.6)	146.3	7.95 d (16.2)
8‴	115.2	6.73 d (15.6)	114.7	6.56 d (16.2)
9‴	167.3		166.8	

were allose and apiose moieties. In the HMBC spectrum, correlations of H-1′ (δ_H 5.31, allose)/α-C (δ_C 71.1, phenylethanol), H-3′ (δ_H 6.50, allose)/C-9‴ (δ_C 167.3, caffeoyl), and H-1″ (δ_H 6.06, apiose)/C-2′ (δ_C 72.2, allose) were also observed. Thus, **7** was determined to be 2-(3,4-dihydroxyphenyl)-ethyl 1-*O*-[3-*O*-caffeoyl-2-*O*-β-D-apiofuranosyl]-β-D-allopyranoside.

The ^{1}H NMR data of compound **8** also indicated the existence of two sets of ABX-type aromatic signals, two *trans*-olefinic protons, a β-methylene and two anomeric protons. The methyl signals at δ_H 1.67 (3H, d, J = 6.6 Hz) indicated the existence of rhamnose. Cross-peaks of H-1′ (δ_H 5.53, allose)/α-C (δ_C 71.6, phenylethanol), H-4′ (δ_H 5.62, allose)/C-9‴ (δ_C 166.8, caffeoyl), and H-1″ (δ_H 5.72, rhamnose)/C-2′ (δ_C 74.0, allose) were observed in HMBC. Thus, **8** was proposed as a 2-(3,4-dihydroxyphenyl)-ethyl 1-*O*-[4-*O*-caffeoyl-2-*O*-α-L-rhamnopyranosyl]-β-D-allopyranoside.

Magnoloside N (**9**) was obtained as a white amorphous powder, displaying a molecular formula of $C_{41}H_{56}O_{25}$ based on HRESIMS m/z 947.2986 $[M-H]^-$ (calcd for $C_{41}H_{55}O_{25}$, 947.3032). The ^{1}H NMR spectrum of **9** had two sets of ABX-type aromatic signals, two *trans*-olefinic protons, a β-methylene and four anomeric proton resonances at δ_H 5.23 (1H, d, J = 8.4 Hz, H-1′), 5.08 (1H, d, J = 7.8 Hz, H-1″), 5.75 (1H, s, H-1‴) and 5.43 (1H, d, J = 7.8 Hz, H-1⁗). The methyl signal at δ_H 1.67 (3H, d, J = 6.0 Hz) indicated the existence of rhamnose. Comparison of the NMR data of **9** with those of magnoloside C (Hasegawa et al., 1988b) suggested **9** contained phenylethanol, caffeoyl, allose, rhamnose and two glucose moieties. In the ^{13}C NMR spectrum of **9**, the presence of only one signal at δ_C 69.4 indicated that the terminal glucose was not linked to C-2″. All connectivities within **9** were established by an HMBC experiment, with correlations of H-1′ (δ_H 5.23, allose)/C-α (δ_C 71.1, phenylethanol), H-3′ (δ_H 6.35, allose)/C-9⁗ (δ_C 167.3, caffeoyl), H-1‴ (δ_H 5.75, rhamnose)/C-2′ (δ_C 72.1, allose), H-1″ (δ_H 5.08, one glucose)/C-6′ (δ_C 69.4, allose), and H-1⁗ (δ_H 5.43, the other glucose)/C-4 (δ_C 145.0, phenylethanol) being observed (Fig. 2). Thus, **9** was deduced to be 2-(3-hydroxy-4-*O*-β-D-glucopyranosylphenyl)-ethyl 1-*O*-[3-*O*-caffeoyl-2-*O*-α-L-rhamnopyranosyl-6-*O*-β-D-glucopyranosyl]-β-D-allopyranoside.

Magnolosides O (**10**) and P (**11**), obtained as white amorphous powders, displayed molecular formulae of $C_{35}H_{48}O_{21}$ and $C_{34}H_{46}O_{20}$ based on HRESIMS m/z 803.2599 $[M-H]^-$ (calcd for $C_{35}H_{47}O_{21}$, 803.2610) and 773.2513 $[M-H]^-$ (calcd for $C_{34}H_{45}O_{20}$, 773.2504), respectively. The ^{1}H NMR spectra of **10** and **11** exhibited a set of ABX-type aromatic signals and a β-methylene moiety, which indicated the existence of a 3,4-dihydroxyphenylethanol group (Table 1). There were also three anomeric proton resonances at δ_H 5.39 (1H, d, J = 7.8 Hz, H-1′), 5.31 (1H, d, J = 7.8 Hz, H-1″), and 6.07 (1H, d, J = 1.2 Hz, H-1‴) in **10** and δ_H 5.39 (1H, d, J = 7.8 Hz, H-1′), 5.28 (1H, d, J = 7.2 Hz, H-1″), and 6.08 (1H, s, H-1‴) in **11**, respectively. The methyl signal at δ_H 1.70 (3H, d, J = 6.6 Hz) in **10** and δ_H 1.62 (3H, d, J = 6.0 Hz) in **11** indicated the existence of a rhamnose moiety. Compared with the NMR data of **1**, allose and glucose moieties were suggested in both **10** and **11**. Additionally, **10** contained a syringoyl group which was indicated by the signals of two equivalent methoxyls δ_H 3.56 (6H, s), two equivalent aromatic protons δ_H 7.50 (2H, s) and one carbonyl carbon δ_C 166.3. The deshielded shift of C-6′ (δ_C 66.2, allose) and C-4‴ (δ_C 84.8, rhamnose) indicated the linkages between syringoyl and C-6′, glucose and C-4‴, respectively, which were confirmed by the correlations of H-6′ (δ_H 5.31, 4.91, allose)/C-7⁗ (δ_C 166.3, syringoyl), H-1″ (δ_H 5.31, glucose)/C-4‴ (δ_C 84.8, rhamnose), H-1‴ (δ_H 6.07, rhamnose)/C-4⁗ (δ_C 139.4, syringoyl), and H-1′ (δ_H 5.39, allose)/C-α (δ_C 71.5, phenylethanol) in HMBC. Thus, **10** was determined to be 2-(3,4-dihydroxyphenyl)-ethyl 1-*O*-{6-*O*-[4-*O*-β-D-glucopyranosyl-(1 → 4)-α-L-rhamnopyranosyl]-syringoyl}-β-D-allopyranoside.

Compared with the NMR data of **10**, an additional set of ABX-type aromatic signals and only one methoxyl were suggested in **11**, which indicated the existence of a vanilloyl group. The methoxyl was assigned to C-3⁗ (δ_C 150.2) aided by the correlation between the protons of methoxyl (δ_H 3.63) and H-2⁗ (δ_H 7.80, d, 1.8 Hz) in NOESY (Fig. 2). Thus compound **11** was assigned as 2-(3,4-dihydroxyphenyl)-ethyl 1-*O*-{6-*O*-[4-*O*-β-D-glucopyranosyl-(1 → 4)-α-L-rhamnopyranosyl]-vanilloyl}-β-D-allopyranoside.

Magnoloside Q (**12**) was obtained as a white amorphous powder, displaying a molecular formula of $C_{27}H_{40}O_{16}$ based on HRESIMS m/z 619.2252 $[M-H]^-$ (calcd for $C_{27}H_{39}O_{16}$, 619.2238). The ^{1}H NMR spectrum of **12** (Table 4) exhibited a set of ABX-type aromatic signals: δ_H 7.01 (1H, d, J = 1.2 Hz), 6.94 (1H, d, J = 8.4 Hz), and 6.90 (1H, dd, J = 8.4, 1.2 Hz). The resonances at δ_H 6.04 (1H, m), 5.10 (2H, m), and 3.34 (2H, d, J = 6.0 Hz) also indicated the presence of an allyl group. Compared with the NMR data of 3,4-dihydroxy-allylbenzene-3-*O*-α-L-rhamnopyranosyl-(1 → 6)-β-D-glucopyranoside (DARG) (Deng et al., 2000), **12** contained the same aglycone as that of DARG. Three anomeric proton resonances at δ_H 5.06 (1H, d, J = 7.2 Hz), 4.69 (1H, d, J = 7.8 Hz), and 4.78 (1H, overlap) indicated the presence of three sugar moieties in **12**. The typical methyl signal at δ_H 1.28 (3H, d, 6.6 Hz) indicated the presence of a rhamnose moiety, and exhaustive acidic hydrolysis confirmed the existence of L-rhamnose and D-glucose. The connected position of the sugar chain on the aglycone was determined by correlation of H-1′ (δ_H 5.06, inner glucose)/C-3 (δ_C 147.3, allylbenzene) in the HMBC spectrum. Simultaneously, correlations of H-6′ (δ_H 4.02, 3.73, inner glucose)/C-1″ (δ_C 103.1, rhamnose) and H-1‴ (δ_H 4.69, terminal glucose)/C-4″ (δ_C 84.1, rhamnose) resolved other connectivities. Thus, **12** was identified as 3,4-dihydroxy-allylbenzene-3-*O*-[6-*O*-β-D-glucopyranosyl-(1 → 4)-α-L-rhamnopyranosyl]-β-D-glucopyranoside.

Table 4
^{1}H (600 MHz) and ^{13}C NMR (150 MHz) spectroscopic data of compounds **12** and **13** in D_2O.

Position	**12**		**13**	
	δ_C	δ_H (J in Hz)	δ_C	δ_H (J in Hz)
1	136.1		136.1	
2	119.7	7.01 d (1.2)	119.7	7.04 d (1.8)
3	147.3		147.4	
4	146.6		146.5	
5	119.4	6.94 d (8.4)	119.3	6.93 d (8.4)
6	126.7	6.90 dd (8.4, 1.2)	126.6	6.89 dd (8.4, 1.8)
7	41.7	3.34 d (6.0)	41.7	3.35 d (6.0)
8	141.2	6.04m	141.2	6.04m
9	118.4	5.10m	118.3	5.11 dd (18.0, 1.2)
				5.10 dd (10.2, 1.2)
All/Glc-1′	103.9	5.06 d (7.2)	102.0	5.31 d (7.8)
2′	75.7	3.64 dd (9.6, 7.2)	72.9	3.81 dd (7.8, 3.0)
3′	78.3	3.61 t (9.6)	73.8	4.29 t (3.0)
4′	72.3	3.54 t (8.4)	69.6	3.80 dd (9.6, 3.0)
5′	77.7	3.72 overlap	75.4	4.05 ddd (9.6, 6.0, 3.0)
6′	69.3	4.02 dd (14.4, 5.4)	69.9	4.00 dd (11.4, 3.0)
		3.73 overlap		3.70 dd (11.4, 6.0)
Rha-1″	103.1	4.78 overlap	103.2	4.78 d (1.8)
2″	72.9	3.95 dd (3.6, 1.2)	72.9	3.95 dd (3.6, 1.8)
3″	73.1	4.00 dd (9.6, 3.6)	73.1	4.01 dd (9.6, 3.6)
4″	84.1	3.66 t (9.6)	84.1	3.66 t (9.6)
5″	70.0	3.79m	70.0	3.79m
6″	19.6	1.28 d (6.6)	19.6	1.28 d (6.6)
Glc-1‴	106.1	4.69 d (7.8)	106.1	4.69 d (7.8)
2‴	76.8	3.31 d (7.8)	76.8	3.31 dd (9.0, 7.8)
3‴	78.7	3.51 t (9.0)	78.6	3.50 t (9.0)
4‴	72.4	3.41 t (9.0)	72.4	3.40 t (9.0)
5‴	78.8	3.44 ddd (9.0, 5.4, 1.8)	78.8	3.43 ddd (9.0, 5.4, 1.8)
6‴	63.5	3.91 dd (12.0, 1.8)	63.5	3.91 dd (12.0, 1.8)
		3.74 dd (12.0, 5.4)		3.74 dd (12.0, 5.4)

Table 5
^{1}H (600 MHz) and ^{13}C NMR (150 MHz) spectroscopic data of compounds **14** and **15** in pyridine-d_5.

Position	**14**		**15**	
	δ_C	δ_H (J in Hz)	δ_C	δ_H (J in Hz)
1	155.1		155.6	
2	95.5	6.74s	95.8	6.97s
3	154.3		154.3	
4	134.1		134.1	
5	154.3		154.3	
6	95.5	6.74s	95.8	6.97s
3,5-OCH_3	56.0	3.71s	56.0	3.75s
4-OCH_3	60.7	3.85s	60.7	3.84s
Glc/All-1′	102.6	5.55 d (7.2)	99.7	6.04 d (7.8)
2′	74.9	4.36 t (9.0)	74.3	4.49 dd (7.8, 3.0)
3′	76.8	4.35 overlap	68.9	5.00 t (3.0)
4′	79.3	4.32 t (9.0)	68.8	4.18 dd (9.6, 3.0)
5′	77.4	4.03m	76.7	4.68m
6′	61.4	4.44 d (12.0)	62.8	4.57 dd (12.0, 2.4)
		4.26 dd (12.0, 5.4)		4.34 dd (12.0, 6.6)
Api-1″	111.1	6.03 d (3.6)	106.3	6.02 brs
2″	77.5	4.84 d (3.6)	77.9	4.69s
3″	80.2		81.0	
4″	75.2	4.80 d (9.6)	75.8	4.86 d (9.0)
		4.36 overlap		4.45 d (9.0)
5″	64.9	4.20 d (11.4)	66.6	4.35 d (11.4)
		4.18 d (11.4)		4.31 d (11.4)

Magnoloside R (**13**) was also a white amorphous powder, and possessed the same molecular formula of $C_{27}H_{40}O_{16}$ as that of **12** based on HRESIMS m/z 619.2242 $[M-H]^-$ (calcd for $C_{27}H_{39}O_{16}$, 619.2238). The ^{1}H and ^{13}C NMR data of **13** (Table 4) were similar to those of **12**. This was supported by the ^{1}H NMR data of a set of ABX-type aromatic protons, allyl protons, three anomeric protons and a typical methyl of rhamnose. However, comparison of the NMR data indicated that the inner glucose moiety in **12** was replaced by an allose group in **13**, which was supported by exhaustive acidic hydrolysis. Correlations (Fig. 2) of H-1′ (δ_H 5.31, allose)/C-3 (δ_C 147.4, allylbenzene), H-6′ (δ_H 4.00, 3.70, allose)/C-1″ (δ_C 103.2, rhamnose), H-4″ (δ_H 3.66, rhamnose)/C-1‴ (δ_C 106.1, glucose) suggested the connectivities. Thus, structure **13** was elucidated as 3,4-dihydroxy-allylbenzene-3-*O*-[6-*O*-*β*-D-glucopyranosyl-(1 → 4)-*α*-L-rhamnopyranosyl]-*β*-D-allopyranoside.

Magnolosides S (**14**) and T (**15**), displayed the same molecular formula $C_{20}H_{30}O_{13}$ based on HRESIMS m/z 477.1617 $[M-H]^-$ (calcd for $C_{20}H_{29}O_{13}$, 477.1608) and 477.1618 $[M-H]^-$ (calcd for $C_{20}H_{29}O_{13}$, 477.1608), respectively. They also possessed the same aglycone of a 3,4,5-trimethoxyphenol group indicated by the ^{1}H NMR data of two equivalent methoxyls at δ_H 3.71 (6H, s) in **14**, 3.75 (6H, s) in **15**, one methoxyl at δ_H 3.85 (3H, s) in **14**, 3.84 (3H, s) in **15** and two equivalent aromatic protons at δ_H 6.74 (2H, s) in **14**, 6.97 (2H, s) in **15**. Two equivalent methoxyls were linked to C-3 and C-5 instead of C-2 and C-6 by comparison with the ^{13}C NMR data of khaephuoside A (Tripetch et al., 2002). Two anomeric proton resonances at δ_H 5.55 (1H, d, J = 7.2 Hz) and 6.03 (1H, d, J = 3.6 Hz) in **14** and δ_H 6.04 (1H, d, J = 7.8 Hz) and 6.02 (1H, brs) in **15** indicated the presence of two sugar moieties. Comparison with the NMR data of **2** suggested the existence of a glucose and an apiose in **14**. The difference between **14** and **15** was that the glucose moiety in **14** was replaced by an allose in **15** which was supported by the signal of H-3′ (δ_H 5.00, t, J = 3.0 Hz, allose). Correlations of H-1″ (δ_H 6.03, apiose)/C-4′ (δ_C 79.3, glucose), H-1′ (δ_H 5.55, glucose)/C-1 (δ_C 155.1, aglycone) in **14** and H-1″ (δ_H 6.02, apiose)/C-2′ (δ_C 74.3, allose), H-1′ (δ_H 6.04, allose)/C-1 (δ_C 155.6, aglycone) in **15** were observed in the HMBC. Accordingly, compounds **14** and **15** were elucidated as 3,4,5-trimethoxyphenyl-1-*O*-[4-*O*-*β*-D-apiofuranosyl]-*β*-D-glucopyranoside, and 3,4,5-trimethoxyphenyl-1-*O*-[2-*O*-*β*-D-apiofuranosyl]-*β*-D-allopyranoside, respectively.

Magnoloside U (**16**), a pale yellow amorphous powder, was assigned the molecular formula $C_{30}H_{40}O_{14}$ from HRESIMS data at m/z 623.2349 $[M-H]^-$ (calcd for $C_{30}H_{39}O_{14}$, 623.2340). Its ^{1}H NMR data indicated the existence of two sets of ABX-type aromatic protons, one allyl moiety and a 1,2-dihydroxypropyl moiety. Compared with the NMR data of 1,1′-dibenzene-6′,8′,9′-trihydroxy-3-allyl-4-*O*-*β*-D-glucopyranoside (Deng et al., 2002), the signal of an additional glucose moiety in compound 16 was observed. Further information was obtained from two anomeric proton resonances at δ_H 5.59 (1H, d, J = 7.2 Hz) and 5.79 (1H, d, J = 7.8 Hz), and the result of exhaustive acidic hydrolysis of **16**, where only glucose was liberated. The connectivities of H-1″ (δ_H 5.59, one glucose)/C-4 (δ_C 155.1, aglycone) and H-1‴ (δ_H 5.79, the other glucose)/C-6′ (δ_C 153.3, aglycone) were established by an HMBC experiment. Thus, **16** was determined as 1,1′-dibenzene-8′,9′-dihydroxy-3-allyl-(6′-*O*-*β*-D-glucopyranosyl)-4-*O*-*β*-D-glucopyranoside.

Magnolosides V (**17**) and W (**18**) were obtained as white amorphous powders, and had the molecular formulae of $C_{36}H_{50}O_{21}$ and $C_{35}H_{48}O_{20}$ based on HRESIMS m/z 817.2749 $[M-H]^-$ (calcd for $C_{36}H_{49}O_{21}$, 817.2766) and 787.2666 $[M-H]^-$ (calcd for $C_{35}H_{47}O_{20}$, 787.2661), respectively. The ^{1}H NMR of **17** (Table 6) exhibited AA′BB′-type aromatic protons at δ_H 7.31 (2H, d, J = 9.0 Hz), 7.27 (2H, d, J = 9.0 Hz), and 1,2-dihydroxypropyl signals at δ_H 3.11 (1H, dd, J = 13.2, 5.4 Hz), 2.97 (1H, dd, J = 13.2, 7.8 Hz), 4.28 (1H, overlap), 4.01 (1H, dd, J = 10.8, 4.2 Hz), and 3.96 (1H, dd, J = 10.8, 6.0 Hz), which suggested that the aglycone was a 4-(1,2-dihydroxypropyl)-phenol (Deng et al., 2002). Comparison of the NMR data of **17** with those of **10** indicated the existence of syringoyl, allose, glucose and rhamnose moieties in **17**. The connectivities of H-1‴ (δ_H 5.30, glucose)/C-4″ (δ_C 84.6, rhamnose), H-1″ (δ_H 6.11, rhamnose)/C-4⁗ (δ_C 139.3, syringoyl), H-6′ (δ_H 5.35, 4.93, allose)/C-7⁗ (δ_C 166.0, syringoyl), H-1′ (δ_H 6.01, allose)/C-1 (δ_C 157.0, aglycone) were established by an HMBC experiment. Accordingly, **17** was confined as 4-(1,2-dihydroxypropyl)-phenyl 1-*O*-{6-*O*-[4-*O*-*β*-D-glucopyranosyl-(1 → 4)-*α*-L-rhamnopyranosyl]-syringoyl}-*β*-D-allopyranoside. The difference between **18** and **17** is that the syringoyl moiety in **17** was replaced by a vanilloyl in **18**, which was supported by the signals of a set of ABX-type aromatic protons and a methoxyl. The methoxyl group was assigned to C-3⁗ (δ_C 150.4), this being aided by the correlation between the protons of methoxyl group (δ_H 3.67) and H-2⁗ (δ_H 7.80, d, J = 1.8 Hz) in NOESY (Fig. 2). Thus, **18** was assigned as 4-(1,2-dihydroxypropyl)-phenyl 1-*O*-{6-*O*-[4-*O*-*β*-D-glucopyranosyl-(1 → 4)-*α*-L-rhamnopyranosyl]-vanilloyl}-*β*-D-allopyranoside.

Magnolosides X (**19**), Y (**20**) and Z (**21**) were isolated as pale yellow amorphous powders, and their molecular formulae were assigned to be $C_{30}H_{40}O_{16}$, $C_{29}H_{38}O_{16}$ and $C_{29}H_{38}O_{15}$ based on the HRESIMS m/z 701.2317 $[M+HCOO]^-$ (calcd for $C_{31}H_{41}O_{18}$, 701.2293), 641.2088 $[M-H]^-$ (calcd for $C_{29}H_{37}O_{16}$, 641.2082), and 671.2215 $[M+HCOO]^-$ (calcd for $C_{30}H_{39}O_{17}$, 671.2187), respectively. The ^{1}H NMR spectrum of **19** (Table 6) exhibited signals for AA′BB′-type aromatic protons, a 1, 2-dihydroxypropyl moiety, a syringoyl moiety and two anomeric proton resonances at δ_H 5.30 (1H, d, J = 7.8 Hz) and 5.40 (1H, s). The NMR data of **19** were similar to those of **17**, except for the absence of a terminal glucose in **19**. The HMBC spectrum established correlations of H-1′ (δ_H 5.30, allose)/C-1 (δ_C 157.6, aglycone) and H-1″ (δ_H 5.40, rhamnose)/C-4‴ (δ_C 140.5, syringoyl). The deshielded shift of C-6′ (δ_C 67.6, allose) showed a lingkage between syringoyl and C-6′. Thus, **19** was assigned as 4-(1, 2-dihydroxypropyl)-phenyl 1-*O*-{6-*O*-[4-*O*-*α*-L-rhamnopyranosyl]-syringoyl}-*β*-D-allopyranoside. The difference between **21** and **19** was that the syringoyl moiety in **19** was replaced by a vanilloyl in **21**, which was supported by the signals of a set of ABX-type aromatic protons and a methoxyl. The methoxyl group was assigned to C-3⁗ (δ_C 151.8) aided by the correlation between protons of methoxyl group (δ_H 3.80) and H-2⁗

Table 6
^{1}H (600 MHz) and ^{13}C NMR (150 MHz) spectroscopic data of compounds **17**–**21**.

Position	**17**[a]		**18**[a]		**19**[b]		**20**[a]		**21**[b]	
	δ_C	δ_H (J in Hz)	δ_C	δ_H (J in Hz)	δ_C	δ_H (J in Hz)	δ_C	δ_H (J in Hz)	δ_C	δ_H (J in Hz)
1	157.0		157.2		157.6		156.9		157.7	
2,6	116.5	7.27 d (9.0)	116.8	7.28 d (8.4)	119.2	6.91 d (7.8)	116.5	7.24 d (8.4)	119.2	6.91 d (8.4)
3,5	130.8	7.31 d (9.0)	131.0	7.34 d (8.4)	133.1	6.88 d (7.8)	130.8	7.29 d (8.4)	133.1	6.89 d (8.4)
4	133.7		133.9		135.5		133.6		135.3	
7	40.1	3.11 dd (13.2, 5.4) 2.97 dd (13.2, 7.8)	40.3	3.10 dd (13.8, 4.8) 2.97 dd (13.8, 7.8)	40.8	2.66 dd (13.8, 4.8) 2.54 dd (13.8, 7.8)	40.0	3.09 dd (13.2, 4.8) 2.96 dd (13.2, 7.8)	40.9	2.65 dd (13.8, 5.4) 2.54 dd (13.8, 7.8)
8	73.8	4.28 overlap	74.0	4.29 overlap	75.6	3.54 t (9.6)	73.9	4.27 overlap	75.6	3.78 overlap
9	66.5	4.01 dd (10.8, 4.2) 3.96 dd (10.8, 6.0)	66.8	4.02 dd (11.4, 4.8) 3.97 dd (11.4, 6.6)	67.7	3.56 overlap 3.43 dd (10.8, 7.2)	66.5	3.98m	67.6	3.56 overlap 3.41 dd (11.4, 6.6)
All-1′	100.2	6.01 d (7.8)	100.3	6.00 d (7.8)	100.7	5.30 d (7.8)	100.0	5.96 d (7.8)	100.6	5.31 d (7.8)
2′	71.8	4.30 overlap	72.4	4.33 overlap	73.8	4.29–4.25 overlap	71.6	4.32–4.29 overlap	73.9	4.28 overlap
3′	72.8	4.87s	73.3	4.29 overlap	73.0	3.82–3.76 overlap	73.1	4.82s	72.9	3.80 overlap
4′	69.2	4.23 overlap	69.4	4.23 overlap	70.7	3.82–3.76 overlap	69.2	4.17 dd (9.0, 3.0)	70.6	3.80 overlap
5′	73.1	4.87 overlap	73.1	4.86 overlap	74.5	4.29–4.25 overlap	72.9	4.32–4.29 overlap	74.4	4.28 overlap
6′	65.9	5.35 d (10.8) 4.93 overlap	65.7	5.31 d (11.4) 4.90 dd (11.4, 7.2)	67.6	4.66 brd (11.4) 4.57 dd (11.4, 8.4)	65.4	5.30 dd (9.6, 5.4) 4.84 overlap	67.3	4.63 brd (11.4) 4.54 dd (11.4, 8.4)
Rha/All-1″	103.1	6.11s	100.4	6.16s	104.7	5.40s	99.5	6.21 d (7.8)	101.6	5.62s
2″	71.4	4.95 overlap	71.4	4.78s	72.9	4.03 brd (9.6)	71.8	4.32–4.29 overlap	72.6	4.25 overlap
3″	72.2	4.31 overlap	72.0	4.32 overlap	73.3	4.26 overlap	73.0	4.80 t (3.0)	73.0	4.05 dd (9.6, 2.4)
4″	84.6	4.51 t (9.0)	84.4	4.49 dd (9.6, 9.0)	74.3	3.79 overlap	68.4	4.32–4.29 overlap	74.7	3.56 dd (9.6, 6.6)
5″	69.5	4.22 overlap	69.3	4.23 overlap	72.8	4.29–4.25 overlap	76.3	4.71 ddd (9.6, 5.4, 2.4)	72.7	3.80 overlap
6″	18.2	1.72 d (6.0)	18.4	1.65 d (6.0)	19.5	1.26 d (6.0)	62.3	4.52 dd (12.6, 2.4) 4.36 dd (12.6, 5.4)	19.6	1.26 d (6.0)
Glc-1‴	106.7	5.30 d (7.8)	106.7	5.28 d (7.8)						
2‴	76.3	4.17 dd (9.0, 7.8)	76.3	4.13 t (8.4)						
3‴	78.3	4.29 overlap	78.5	4.22 t (9.0)						
4‴	71.2	4.31 overlap	71.3	4.33 t (9.0)						
5‴	78.4	3.83m	78.6	3.80 ddd (9.0, 4.8, 2.4)						
6‴	62.4	4.47 dd (11.4, 1.2) 4.40 dd (11.4, 4.2)	62.6	4.44 dd (12.0, 2.4) 4.38 dd (12.0, 4.8)						
1⁗	126.3		125.0		128.8		123.9		126.9	
2⁗	107.3	7.51s	113.9	7.80 d (1.8)	110.0	7.27s	113.4	7.77 d (1.8)	116.3	7.50s
3⁗	153.5		150.4		155.4		149.4		151.8	
4⁗	139.3		150.6		140.5		151.9		151.7	
5⁗	153.5		116.9	7.53 d (8.4)	155.4		114.8	7.56 overlap	119.0	7.25 d (8.4)
6⁗	107.3	7.51s	123.9	7.91 dd (8.4, 1.8)	110.0	7.27s	123.8	7.80 dd (8.4, 1.8)	126.7	7.60 brd (8.4)
7⁗	166.0		166.3		170.0		166.1		170.2	
OCH_3	55.9	3.60s	56.0	3.67s	59.0	3.83s	55.6	3.63s	58.8	3.80s

[a] Recorded in pyridine-d_5.
[b] Recorded in D_2O.

(δ_H 7.50, s) in NOESY. So, **21** was assigned as 4-(1, 2-dihydroxypropyl)-phenyl 1-*O*-{6-*O*-[4-*O*-α-*L*-rhamnopyranosyl]-vanilloyl}-β-*D*-allopyranoside. The NMR data of **20** were similar to those of **21**, except for signals H-1″ (δ_H 6.21, d, J = 7.8 Hz) and H-3″ (δ_H 4.80, t, J = 3.0 Hz) from an additional allose instead of a rhamnose. The HMBC spectrum established the connectivities of H-1′ (δ_H 5.96, inner allose)/C-1 (δ_C 156.9, aglycone), H-6′ (δ_H 5.30, 4.84, inner allose)/C-7‴ (δ_C 166.1, vanilloyl), and H-1″ (δ_H 6.21, terminal allose)/C-4‴ (δ_C 151.9, vanilloyl). Thus, **20** was assigned as 4-(1, 2-dihydroxypropyl)-phenyl 1-*O*-{6-*O*-[4-*O*-β-*D*-allopyranosyl]-vanilloyl}-β-*D*-allopyranoside.

2.2. α-glucosidase inhibitory effects and cytotoxicity

α-Glucosidase inhibitors (e.g., acarbose, miglitol and voglibose) are widely used in the treatment of type-2 diabetes. They have various side-effects such as liver toxicity and adverse gastrointestinal symptoms, thereby raising the risk factors of heart disease (Tewari et al., 2003). Therefore, safer natural α-glucosidase inhibitors are needed and many compounds have been reported from plant sources (Jabeen et al., 2013; Liu et al., 2014; Ying et al., 2014). Of these, stewartiiside, a phenylethanoid glycoside, was reported to be a better α-glucosidase inhibitor than acarbose (Jabeen et al., 2013). In the present study, the isolated compounds were evaluated for their α-glucosidase inhibitory effects, and acarbose was used as a positive control (Jabeen et al., 2013). Compounds **4**, **6** and **22** showed strong inhibition (IC_{50} 0.13, 0.27 and 0.29 mM respectively), whereas compounds **1**, **3**, **19**, **21** and **23**–**26** exhibited moderate inhibition (IC_{50} in the range 0.51–0.94 mM) compared to acarbose (IC_{50} 1.09 mM) (Table 7). The above compounds are all phenylethanoid glycosides. Conversely, the phenolic glycosides **12**–**15** and **17** exhibited inhibitory rate less than 50% at a concentration of 1.0 mM. This result suggested that phenylethanoid glycosides have stronger inhibitory activities than those of phenolic glycosides, whereas the contribution of coumaroyl, feruloyl, and caffeoyl groups decreased.

According to the result of a network pharmacological study (data not shown), the isolated compounds were predicted to have cytotoxic activities. In addition, several phenylethanoid glycosides were reported to possess cytotoxic activity (Argyropoulou et al., 2012; Harput et al., 2012; Hwang et al., 2011; Yang et al., 2011). Accordingly, the cytotoxicity of the isolated compounds against stomach cancer (MGC-803), liver cancer (HepG2), prostate cancer (PC3), breast cancer (MCF-7), PC12 cell strain, lung cancer (A549) and normal kidney cells (Vero) were evaluated using a MTT assay (Monks et al., 1991). Being a widely used broad-spectrum antitumor drug, fluorouracil (5-FU) was chosen as a positive control (Guo et al., 2014). Glycosides **1**–**3**, **5**–**7**, **10**–**11** and **22**–**26** showed moderate cytotoxicity against MGC-803 and HepG2, while phenolic glycosides **12**–**16**, **19**, **21** and **27**–**29** showed no cytotoxicity

Table 7
Inhibitory effects of isolated compounds against α-glucosidase.[a]

Compounds	IC_{50} (mM)	Compounds	IC_{50} (mM)	Compounds	IC_{50} (mM)
1	0.73 ± 0.03	**10**	–	**19**	0.94 ± 0.02
2	0.78 ± 0.04	**11**	–	**20**	–
3	0.51 ± 0.09	**12**	N[c]	**21**	0.94 ± 0.02
4	0.13 ± 0.01	**13**	N	**22**	0.29 ± 0.02
5	–[b]	**14**	N	**23**	0.75 ± 0.17
6	0.27 ± 0.01	**15**	N	**24**	0.62 ± 0.02
7	0.68 ± 0.01	**16**	1.00 ± 0.06	**25**	0.69 ± 0.02
8	–	**17**	N	**26**	0.69 ± 0.10
9	–	**18**	–	Acarbose	1.09 ± 0.04

[a] Each value represents the mean ± SD ($n = 3$).
[b] Not determined.
[c] Exhibit inhibitory effect of <50% at concentration of 1 mM.

against MGC-803 and HepG2. Among the phenylethanoid glycosides, compounds **3**, **23** and **26** exhibited preferable cytotoxic activity against MGC-803 with IC_{50} of 13.59–17.16 μM. Additionally, they exhibited certain cytotoxic activities against HepG2 with IC_{50} of 29.53–32.46 μM and had no cytotoxicity on Vero. Except for compounds **23** and **26**, all the evaluated compound showed no cytotoxicity against PC3, MCF-7, PC12 and A549 (Table 8).

3. Conclusions

Eleven new phenylethanoid glycosides, magnolosides F–P (**1**–**11**), and ten new phenolic glycosides, magnolosides Q–Z (**12**–**21**), along with eight known compounds were isolated from the water-soluble portion of the 70% aq. ethanol extract of the stem bark of *M. officinalis*. Their structures were elucidated by a combination of 1D (^1H, ^{13}C NMR and DEPT), 2D (HSQC, HMBC, and NOESY) NMR spectroscopy, mass spectrometry (ESIMS, HRESIMS), GC and chemical hydrolysis methods and in comparison with literature data. The large number of glycosides isolated and identified further fully indicated the ubiquity of glycosides in *M. officinalis*. Above all, the most common forms isolated were the allopyranosides, which are rare in the plant kingdom. In addition, magnolosides A-B had potent anti-spasmodic activity (Yu et al., 2012) and the present paper showed that large number of phenylethanoid glycosides existed in Houpo, which indicated phenylethanoid glycosides were one of the active constituents to regulate the motility of gastrointestinal tract. Most evaluated phenylethanoid glycosides showed good α-glucosidase inhibitory effects with IC_{50} values ranging between 0.13 and 0.94 mM and moderate cytotoxicity against human cancer cell lines MGC-803 and HepG2 with IC_{50} values of 13.59–54.00 μM, 27.58–63.82 μM, respectively. The results indicated the isolated compounds were one of the active constituents in Houpo.

4. Experimental

4.1. General experimental procedures

Optical rotations were measured on an Automatic Polarimeter (Rudolph, USA). UV spectra were obtained in MeOH on a Jasco V-650 spectrophotometer (JASCO). IR spectra were recorded in KBr pellets on a Bruker VERTEX70 (Bruker, Germany). HRESIMS were obtained on a Waters Xevo G2-XS Q-TOF LC-MS (Waters, USA). ^1H and ^{13}C NMR spectra were taken on a Bruker AVIIIHD 600 spectrometer with the solvent peak used as references (Ettlingen, Germany). Medium pressure liquid chromatography

Table 8
Cytotoxicity of isolated compounds against MGC-803, HepG2, PC3, MCF-7, PC12, A549 and Vero.

Compounds	MGC-803 IC_{50} (μmol)	HepG2 IC_{50} (μmol)	PC3 IC_{50} (μmol)	MCF-7 IC_{50} (μmol)	PC12 IC_{50} (μmol)	A549 IC_{50} (μmol)	Vero IC_{50} (μmol)
1	21.39 ± 1.08	27.58 ± 1.98	>100	>100	>100	>100	43.42 ± 1.54
2	38.51 ± 3.21	38.90 ± 2.20	>100	>100	>100	>100	>100
3	13.59 ± 1.78	32.46 ± 5.31	>100	>100	>100	>100	>100
5	49.77 ± 5.12	58.38 ± 3.33	>100	>100	>100	>100	>100
6	38.40 ± 3.23	48.82 ± 2.20	>100	>100	>100	>100	>100
7	26.51 ± 3.11	32.18 ± 2.76	>100	>100	>100	>100	>100
10	45.24 ± 3.45	54.88 ± 4.32	>100	>100	>100	>100	>100
11	54.00 ± 4.23	63.82 ± 8.89	>100	>100	>100	>100	>100
12	>100	>100	>100	>100	>100	>100	>100
13	>100	>100	>100	>100	>100	>100	>100
14	>100	>100	>100	>100	>100	>100	>100
15	>100	>100	>100	>100	>100	>100	>100
16	>100	>100	>100	>100	>100	>100	>100
19	>100	>100	>100	>100	>100	>100	>100
21	>100	>100	>100	>100	>100	>100	>100
22	35.31 ± 2.35	52.20 ± 5.78	>100	>100	>100	>100	>100
23	17.16 ± 2.56	31.26 ± 2.18	>100	>100	99.79 ± 6.95	75.11 ± 5.90	>100
24	24.79 ± 3.45	32.62 ± 4.32	>100	>100	>100	>100	>100
25	21.81 ± 4.31	28.05 ± 1.93	>100	>100	>100	>100	60.21 ± 2.94
26	14.60 ± 2.33	29.53 ± 3.29	98.43 ± 6.21	>100	88.14 ± 7.75	47.12 ± 1.89	>100
27	>100	>100	>100	>100	>100	>100	>100
28	>100	>100	>100	>100	>100	>100	>100
29	>100	>100	>100	>100	>100	>100	>100
5-FU	4.31 ± 1.34	8.57 ± 2.43	31.63 ± 4.32	1.70 ± 3.49	41.52 ± 5.13	24.95 ± 1.81	16.76 ± 2.33

(MPLC) was performed on an EZ Purifier II flash chromatography system (Shanghai Li Sui E-Tech CO. Ltd, Shanghai, China). Analytical HPLC was conducted on a Waters 2695 pump system equipped with a Waters 2996 photodiode array detector (Waters, Milford, MA, USA). Preparative HPLC was performed using a Waters 600 pump, equipped with a Waters 2487 detector. GC was carried out on an Agilent 7890 GC system (Agilent, Santa Clara, CA, USA). Macroporous resin D101 (Tianjin, China), MCI CHP-20P (75–150 μm, Mitsubishi Chemical Corp., Tokyo, Japan), C_{18} (40–60 μm, YMC, Kyoto, Japan), Sephadex LH-20 (Pharmacia, Sweden) and semipreparative column (50 × 250 mm, 10 μm, Agela) were used for column chromatography (CC) separations.

4.2. Plant material

M. officinalis was collected from Enshi city, Hubei Province, People's Republic of China, in May 2009, and identified by Prof. Bin Yang. A voucher specimen (NO. 20090518) is deposited in the Institute of Chinese Materia Medica, China Academy of Chinese Medical Sciences.

4.3. Extraction and isolation

Stem bark (40 kg) was suspended in EtOH:H_2O (40 L, 70:30 v/v) with the bark material extracted by heating the suspension until reflux began (being held for 3 h at this temperature), with this protocol being carried out a further 2×. The combined extracts were dried and then partitioned with EtOAc (3 × 30 L). The water-soluble portion (20 L) was subjected to D101 macroporous resin CC eluted with EtOH:H_2O (0:100 to 95:5), to obtain five fractions (Fr. 1–Fr. 5). Fr. 2 (550 g), eluted using EtOH:H_2O (20:80) was applied to a MCI CHP-20P column eluted with EtOH:H_2O (0:100 to 100:0) to yield four fractions (Fr. 2.1–Fr. 2.4). Fr. 2.1 (170 g, EtOH:H_2O (15:85)) was also applied to a C_{18} CC to yield three major sub-fractions (Fr. 2.1.1–Fr. 2.1.3). Fr. 2.1.1 was re-applied to the C_{18} CC procedure, giving four fractions (Fr. 2.1.1.1–Fr. 2.1.1.4). Fr. 2.1.1.2 was subjected to Sephadex LH–20 CC to yield six fractions (Fr. 2.1.1.2.1–Fr. 2.1.1.2.6). Fr. 2.1.1.2.2 was purified by semi-preparative HPLC using MeOH:H_2O containing 0.1% HCO_2H (20:80, v/v) as eluent, 60 mL/min, giving **14** (71.3 mg, t_R = 49.85 min) and **15** (18 mg, t_R = 46.15 min). Fr. 2.1.1.2.4 was subjected to semi-preparative HPLC, giving four fractions (Fr. 2.1.1.2.4.1–Fr. 2.1.1.2.4.4). Fr. 2.1.1.2.4.3 was re-applied to the semi-preparative HPLC system using MeOH:H_2O containing 0.1% HCO_2H (18:82, v/v) as eluent, 60 mL/min, giving **9** (10.3 mg, t_R = 105.13 min). Fr. 2.1.1.2.4.4 was purified by semi-preparative HPLC with MeOH:H_2O containing 0.1% HCO_2H (23:77, v/v) as eluent, 60 mL/min, giving **16** (34.8 mg, t_R = 41.55 min), **20** (5.56 mg, t_R = 39.17 min). Fr. 2.1.1.2.5 was applied to semi-preparative HPLC, giving four fractions (Fr. 2.1.1.2.5.1–Fr. 2.1.1.2.5.4). Fr. 2.1.1.2.5.4 was re-applied to the semi-preparative HPLC system with MeOH:H_2O containing 0.1% HCO_2H (10:90, v/v) as eluent, 60 mL/min, giving **25** (49 mg, t_R = 69.76 min). Fr. 2.1.3 was applied to Sephadex LH–20 CC to yield five fractions (Fr. 2.1.3.1–Fr. 2.1.3.5). Fr. 2.1.3.4 was purified by semi-preparative HPLC with MeCN:H_2O containing 0.1% HCO_2H (12:88, v/v) as eluent, 60 mL/min, giving **22** (119.6 mg, t_R = 115.83 min). Fr. 2.1.3.5 was purified by semi-preparative HPLC with MeCN:H_2O containing 0.1% HCO_2H (12:88, v/v) as eluent, 60 mL/min, giving **1** (216.6 mg, t_R = 54.39 min), **2** (48.8 mg, t_R = 51.89 min), and **3** (44.6 mg, t_R = 41.00 min). Fr. 2.2 (140 g, EtOH:H_2O (20:80)) was subjected to MPLC with C_{18} CC to yield three major sub-fractions (Fr. 2.2.1–Fr. 2.2.3). Fr. 2.2.2 was applied to Sephadex LH–20 CC, giving eight fractions (Fr. 2.2.2.1–Fr. 2.2.2.8). Fr. 2.2.2.1 was purified by semi-preparative HPLC with MeCN:H_2O containing 0.1% HCO_2H (15:85, v/v) as eluent, 60 mL/min, giving **18** (12.4 mg, t_R = 27.18 min), **17** (5.3 mg, t_R = 32.85 min), **21** (76.1 mg, t_R = 34.69 min), **19** (56.0 mg, t_R = 38.05 min), **12** (197.3 mg, t_R = 49.79 min), **13** (553.4 mg, t_R = 53.58 min), and **27** (38.8 mg, t_R = 48.00 min). Fr. 2.2.2.2 was subjected to semi-preparative HPLC to yield six fractions (Fr. 2.2.2.2.1–Fr. 2.2.2.2.6). Fr. 2.2.2.2.1 was re-applied to the semi-preparative HPLC with MeOH:H_2O containing 0.1% HCO_2H (35:65, v/v) as eluent, 60 mL/min, giving **11** (29.0 mg, t_R = 23.26 min). Compound **10** was obtained from Fr. 2.2.2.2.6 by semi-preparative HPLC with MeCN:H_2O containing 0.1% HCO_2H (15:85, v/v) as eluent. Fr. 2.2.2.5 was purified by semi-preparative HPLC with MeCN:H_2O containing 0.1% HCO_2H (15:85, v/v) as eluent, 60 mL/min, giving **8** (7.0 mg, t_R = 70.69 min). Fr. 2.3 (90 g, EtOH:H_2O (25:75)) was subjected to C_{18} CC to yield three major subfractions (Fr. 2.3.1–Fr. 2.3.3). Fr. 2.3.1 was applied to Sephadex LH-20 CC, giving eight fractions (Fr. 2.3.1.1–Fr. 2.3.1.8). Fr. 2.3.1.4 was subjected to semi-preparative HPLC to yield four fraction (Fr. 2.3.1.4.1–Fr. 2.3.1.4.4), Fr. 2.3.1.4.2 was purified by semi-preparative HPLC with MeCN:H_2O containing 0.1% HCO_2H (12:88, v/v) as eluent, 60 mL/min, giving **4** (21.9 mg, t_R = 75.50 min) and **5** (14.9 mg, t_R = 87.68 min). Fr. 2.3.1.4.3 was purified by semi-preparative HPLC with the same eluent, giving **6** (39.0 mg, t_R = 77.71 min). Fr. 2.3.1.5 was subjected to semi-preparative HPLC using MeOH:H_2O containing 0.1% HCO_2H (25:75, v/v) as eluent, 60 mL/min to yield **7** (100 mg, t_R = 64.61 min) and **24** (2.9 g, t_R = 51.43 min). Fr. 2.4 (105 g, EtOH eluent) was subjected to C_{18} CC to yield four major sub-fractions (Fr. 2.4.1–Fr. 2.4.4). Fr. 2.4.3 was applied to Sephadex LH–20 CC, giving two fractions (Fr. 2.4.3.1–Fr. 2.4.3.2). Fr. 2.4.3.2 was subjected to semi-preparative HPLC with MeOH:H_2O containing 0.1% HCO_2H (40:60, v/v) as eluent, 60 mL/min to yield **23** (206 mg, t_R = 54.33 min).

4.3.1. Magnoloside F (*1*)

Pale yellow amorphous solid; $[\alpha]_D^{20}$ −61.0 (*c* 0.16, MeOH); UV (H_2O) λ_{max} (log ε) 288 (4.47), 330 (4.52) nm; IR (KBr) ν_{max} 3407, 2932, 1693, 1630, 1603, 1523, 1447, 1282, 1041 cm^{-1}; For ^1H NMR (600 MHz, C_5D_5N) and ^{13}C NMR (150 MHz, C_5D_5N) spectroscopic data, see Tables 1 and 2; ESIMS *m/z* 785.1 $[M-H]^-$; HRESIMS *m/z* 785.2496 $[M-H]^-$ (calcd for $C_{35}H_{45}O_{20}$, 785.2504).

4.3.2. Magnoloside G (*2*)

Pale yellow amorphous solid; $[\alpha]_D^{20}$ −35.7 (*c* 0.08, MeOH); UV (H_2O) λ_{max} (log ε) 288 (4.13), 328 (4.27) nm; IR (KBr) ν_{max} 3422, 1692, 1629, 1604, 1522, 1446, 1281, 1043 cm^{-1}; For ^1H NMR (600 MHz, C_5D_5N) and ^{13}C NMR (150 MHz, C_5D_5N) spectroscopic data, see Tables 1 and 2; ESIMS *m/z* 771.0 $[M-H]^-$; HRESIMS *m/z* 771.2328 $[M-H]^-$ (calcd for $C_{34}H_{43}O_{20}$, 771.2348).

4.3.3. Magnoloside H (*3*)

Pale yellow amorphous solid; $[\alpha]_D^{20}$ −25.3 (*c* 0.16, MeOH); UV (H_2O) λ_{max} (log ε) 288 (4.12), 328 (4.09) nm; IR (KBr) ν_{max} 3422, 2936, 1700, 1600, 1358, 1272, 1158, 1044 cm^{-1}; For ^1H NMR (600 MHz, C_5D_5N) and ^{13}C NMR (150 MHz, C_5D_5N) spectroscopic data, see Tables 1 and 2; ESIMS *m/z* 771.1 $[M-H]^-$; HRESIMS *m/z* 771.2334 $[M-H]^-$ (calcd for $C_{34}H_{43}O_{20}$, 771.2348).

4.3.4. Magnoloside I (*4*)

Pale yellow amorphous solid; $[\alpha]_D^{20}$ −54.1 (*c* 0.15, MeOH); UV (H_2O) λ_{max} (log ε) 290 (4.25), 310 (4.29) nm; IR (KBr) ν_{max} 3415, 2933, 1700, 1629, 1604, 1515, 1160, 1043 cm^{-1}; For ^1H NMR (600 MHz, C_5D_5N) and ^{13}C NMR (150 MHz, C_5D_5N) spectroscopic data, see Tables 1 and 2; ESIMS *m/z* 774.3 $[M+NH_4]^+$, 755.1 $[M-H]^-$; HRESIMS *m/z* 755.2377 $[M-H]^-$ (calcd for $C_{34}H_{43}O_{19}$, 755.2399).

4.3.5. Magnoloside J (*5*)

Pale yellow amorphous solid, $[\alpha]_D^{20}$ +25.6 (*c* 0.08, MeOH); UV (H_2O) λ_{max} (log ε) 285 (4.16), 324 (4.17) nm; IR (KBr) ν_{max} 3421,

2933, 1697, 1629, 1599, 1274, 1159, 1046 cm^{-1}; For ^1H NMR (600 MHz, C_5D_5N) and ^{13}C NMR (150 MHz, C_5D_5N) spectroscopic data, see Tables 1 and 2; ESIMS *m/z* 818.3 $[M+NH_4]^+$, 799.1 $[M-H]^-$; HRESIMS *m/z* 799.2651 $[M-H]^-$ (calcd for $C_{36}H_{47}O_{20}$, 799.2661).

*4.3.6. Magnoloside K (**6**)*

Pale yellow amorphous solid; $[\alpha]_D^{20}$ −59.5 (*c* 0.08, MeOH); UV (H_2O) λ_{max} (log ε) 290 (4.18), 328 (4.32) nm; IR (KBr) ν_{max} 3422, 2934, 1700, 1629, 1600, 1517, 1273, 1046 cm^{-1}; For ^1H NMR (600 MHz, C_5D_5N) and ^{13}C NMR (150 MHz, C_5D_5N) spectroscopic data see Tables 1 and 2; ESIMS *m/z* 823.0 $[M+Na]^+$, 798.7 $[M-H]^-$; HRESIMS *m/z* 799.2650 $[M-H]^-$ (calcd for $C_{36}H_{47}O_{20}$, 799.2661).

*4.3.7. Magnoloside L (**7**)*

Pale yellow amorphous solid; $[\alpha]_D^{20}$ −82.4 (*c* 0.09, MeOH); UV (H_2O) λ_{max} (log ε) 290 (4.13), 326 (4.24) nm; IR (KBr) ν_{max} 3385, 1696, 1629, 1605, 1523, 1447, 1282, 1159 cm^{-1}; For ^1H NMR (600 MHz, C_5D_5N) and ^{13}C NMR (150 MHz, C_5D_5N) spectroscopic data, see Table 3; ESIMS *m/z* 633.0 $[M+Na]^+$, 608.8 $[M-H]^-$; HRESIMS *m/z* 609.1817 $[M-H]^-$ (calcd for $C_{28}H_{33}O_{15}$, 609.1819).

*4.3.8. Magnoloside M (**8**)*

Pale yellow amorphous solid; For ^1H NMR (600 MHz, C_5D_5N) and ^{13}C NMR (150 MHz, C_5D_5N) spectroscopic data, see Table 3; ESIMS *m/z* 623.1 $[M-H]^-$; HRESIMS *m/z* 623.1979 $[M-H]^-$ (calcd for $C_{29}H_{35}O_{15}$, 623.1976).

*4.3.9. Magnoloside N (**9**)*

White amorphous solid; ^1H NMR (600 MHz, C_5D_5N) δ 7.92 (1H, d, *J* = 15.6 Hz, H-7‴″), 7.51 (1H, d, *J* = 1.8 Hz, H-2‴″), 7.49 (1H, d, *J* = 7.8 Hz, H-5), 7.26 (1H, d, *J* = 1.8 Hz, H-2), 7.22 (1H, overlap, H-5‴″), 7.07 (1H, dd, *J* = 8.4, 1.8 Hz, H-6‴″), 6.78 (1H, dd, *J* = 7.8, 1.8 Hz, H-6), 6.68 (1H, d, *J* = 15.6 Hz, H-8‴″), 6.35 (1H, t, *J* = 2.4 Hz, H-3′), 5.75 (1H, s, H-1‴), 5.43 (1H, d, *J* = 7.8 Hz, H-1‴′), 5.23 (1H, d, *J* = 8.4 Hz, H-1′), 5.08 (1H, d, *J* = 7.8 Hz, H-1″), 4.78 (1H, brd, *J* = 9.0 Hz, H-6a′), 4.72 (1H, m, H-5‴), 4.54 (1H, overlap, H-2′), 4.53 (2H, m, H-6″), 4.51 (1H, overlap, H-4″), 4.43 (1H, overlap, H-4′), 4.41 (2H, m, H-6‴′), 4.39 (1H, m, H-2‴), 4.34 (1H, overlap, H-4‴), 4.32 (1H, brd, *J* = 9.0 Hz, H-6b′), 4.32–4.22 (2H, m, H-3″, H-3‴′), 4.31 (1H, overlap, H-8a), 4.30 (1H, t, *J* = 7.8 Hz, H-4‴′), 4.21 (2H, m, H-3‴, H-2‴′), 4.08 (1H, t, *J* = 7.8 Hz, H-2″), 4.01 (1H, m, H-5′), 4.00 (1H, m, H-5‴′), 3.93 (1H, m, H-5″), 3.75 (1H, m, H-8b), 3.03 (2H, t, *J* = 7.2 Hz, H-7), 1.67 (3H, d, 6.0 Hz, H-6‴); ^{13}C NMR (150 MHz, C_5D_5N) δ 167.3 (C-9‴″), 150.2 (C-4‴″), 149.1 (C-3), 147.4 (C-3‴″), 145.8 (C-7‴″), 145.0 (C-4), 135.3 (C-1), 126.6 (C-1‴″), 122.0 (C-6‴″), 120.4 (C-6), 119.6 (C-5), 117.9 (C-2), 116.4 (C-5‴″), 115.7 (C-2‴″), 115.0 (C-8‴″), 105.5 (C-1″), 104.8 (C-1‴′), 100.4 (C-1′), 97.8 (C-1‴), 78.8 (C-5‴′), 78.3 (C-5″), 78.2 (C-3″, C-3‴′), 75.0 (C-2″), 74.9 (C-5′), 74.8 (C-2‴′), 73.8 (C-4‴), 72.3 (C-4″), 72.1 (C-2′), 71.8 (C-4‴′), 71.4 (C-3‴), 71.1 (C-8), 71.0 (C-2‴), 70.2 (C-3′), 69.5 (C-5‴), 69.4 (C-6′), 66.2 (C-4′), 62.4 (C-6″), 62.1 (C-6‴′), 36.2 (C-7), 18.5 (C-6‴). ESIMS *m/z* 946.7 $[M-H]^-$; HRESIMS *m/z* 947.2986 $[M-H]^-$ (calcd for $C_{41}H_{55}O_{25}$, 947.3032).

*4.3.10. Magnoloside O (**10**)*

White amorphous solid; $[\alpha]_D^{20}$ −75.5 (*c* 0.21, MeOH); UV (H_2O) λ_{max} (log ε) 268 (4.01) nm; IR (KBr) ν_{max} 3423, 2937, 1705, 1594, 1417, 1338, 1127, 1035 cm^{-1}; For ^1H NMR (600 MHz, C_5D_5N) and ^{13}C NMR (150 MHz, C_5D_5N) spectroscopic data, see Tables 1 and 2; ESIMS *m/z* 822.3 $[M+NH_4]^+$, 803.1 $[M-H]^-$; HRESIMS *m/z* 803.2599 $[M-H]^-$ (calcd for $C_{35}H_{47}O_{21}$, 803.2610).

*4.3.11. Magnoloside P (**11**)*

White amorphous solid; $[\alpha]_D^{20}$ −68.0 (*c* 0.21, MeOH); UV (H_2O) λ_{max} (log ε) 258 (4.22), 287 (3.98) nm; IR (KBr) ν_{max} 3414, 2934, 1702, 1601, 1510, 1289, 1032 cm^{-1}; For ^1H NMR (600 MHz, C_5D_5N) and ^{13}C NMR (150 MHz, C_5D_5N) spectroscopic data, see Tables 1 and 2; ESIMS *m/z* 797.0 $[M+Na]^+$, 772.7 $[M-H]^-$; HRESIMS *m/z* 773.2513 $[M-H]^-$ (calcd for $C_{34}H_{45}O_{20}$, 773.2504).

*4.3.12. Magnoloside Q (**12**)*

White amorphous solid; $[\alpha]_D^{20}$ −85.7 (*c* 0.11, MeOH); UV (H_2O) λ_{max} (log ε) 278 (3.51) nm; IR (KBr) ν_{max} 3417, 2930, 1599, 1540, 1384, 1066 cm^{-1}; For ^1H NMR (600 MHz, D_2O) and ^{13}C NMR (150 MHz, D_2O) spectroscopic data, see Table 4; ESIMS *m/z* 619.1 $[M-H]^-$; HRESIMS *m/z* 619.2252 $[M-H]^-$ (calcd for $C_{27}H_{39}O_{16}$, 619.2238).

*4.3.13. Magnoloside R (**13**)*

White amorphous solid; $[\alpha]_D^{20}$ −82.6 (*c* 0.23, MeOH); UV (H_2O) λ_{max} (log ε) 278 (3.56) nm; IR (KBr) ν_{max} 3406, 2928, 1599, 1540, 1384, 1072 cm^{-1}; For ^1H NMR (600 MHz, D_2O) and ^{13}C NMR (150 MHz, D_2O) spectroscopic data, see Table 4; ESIMS *m/z* 619.1 $[M-H]^-$; HRESIMS *m/z* 619.2242 $[M-H]^-$ (calcd for $C_{27}H_{39}O_{16}$, 619.2238).

*4.3.14. Magnoloside S (**14**)*

Pale yellow amorphous solid, $[\alpha]_D^{20}$ −55.6 (*c* 0.20, MeOH); UV (H_2O) λ_{max} (log ε) 270 (3.39) nm; IR (KBr) ν_{max} 3373, 2939, 1602, 1509, 1221, 1129, 996 cm^{-1}; For ^1H NMR (600 MHz, C_5D_5N) and ^{13}C NMR (150 MHz, C_5D_5N) spectroscopic data, see Table 5; ESIMS *m/z* 979.0 $[2M+Na]^+$, 954.5 $[2M-H]^-$; HRESIMS *m/z* 477.1617 $[M-H]^-$ (calcd for $C_{20}H_{29}O_{13}$, 477.1608).

*4.3.15. Magnoloside T (**15**)*

Pale yellow amorphous solid; $[\alpha]_D^{20}$ −69.6 (*c* 0.16, MeOH); UV (H_2O) λ_{max} (log ε) 275 (3.23) nm; IR (KBr) ν_{max} 3419, 2938, 1602, 1507, 1228, 1126 cm^{-1}; For ^1H NMR (600 MHz, C_5D_5N) and ^{13}C NMR (150 MHz, C_5D_5N) spectroscopic data, see Table 5; ESIMS *m/z* 979.0 $[2\ M+Na]^+$, 954.6 $[2\ M-H]^-$; HRESIMS *m/z* 477.1618 $[M-H]^-$ (calcd for $C_{20}H_{29}O_{13}$, 477.1608).

*4.3.16. Magnoloside U (**16**)*

Pale yellow amorphous solid; $[\alpha]_D^{20}$ −44.4 (*c* 0.20, MeOH); UV (H_2O) λ_{max} (log ε) 253 (4.20), 284 (4.08) nm; IR (KBr) ν_{max} 3406, 2927, 1630, 1603, 1509, 1074 cm^{-1}; ^1H NMR (C_5D_5N, 600 MHz) δ 7.88 (1H, d, *J* = 2.4 Hz, H-2), 7.71 (1H, dd, *J* = 8.4, 2.4 Hz, H-6), 7.61 (1H, d, *J* = 8.4 Hz, H-5′), 7.59 (1H, s, H-2′), 7.51 (1H, d, *J* = 8.4 Hz, H-5), 7.39 (1H, dd, *J* = 8.4, 2.4 Hz, H-4′), 6.24 (1H, m, H-8), 5.79 (1H, d, *J* = 7.8 Hz, H-1‴), 5.59 (1H, d, *J* = 7.2 Hz, H-1″), 5.14 (1H, dd, *J* = 17.4, 1.2 Hz, H-9a), 4.97 (1H, brd, *J* = 10.2 Hz, H-9b), 4.55 (1H, dd, *J* = 12.0, 2.4 Hz, H-6a″), 4.52 (1H, dd, *J* = 12.0, 2.4 Hz, H-6a‴), 4.46–4.36 (1H, m, H-5‴), 4.45 (1H, overlap, H-2‴), 4.40 (2H, overlap, H-6b″, H-6b‴), 4.39 (3H, overlap, H-8′, H-4″, H-4‴), 4.27 (1H, m, H-2″), 4.15–4.12 (3H, m, H-3″, H-5″, H-3‴), 4.07 (2H, m, H-9′), 3.73 (1H, dd, *J* = 15.0, 9.0 Hz, H-7a), 3.62 (1H, dd, *J* = 15.0, 6.6 Hz, H-7b), 3.23 (1H, dd, *J* = 13.2, 4.8 Hz, H-7a′), 3.11 (1H, dd, *J* = 13.2, 7.2 Hz, H-7b′); ^{13}C NMR (C_5D_5N, 150 MHz) δ 155.1 (C-4), 153.3 (C-6′), 137.6 (C-8), 133.5 (C-3′), 132.8 (C-1), 132.4 (C-2′), 131.7 (C-2), 130.6 (C-1′), 129.5 (C-4′), 129.1 (C-6), 128.9 (C-3), 115.3 (C-9), 114.7 (C-5, C-5′), 102.3 (C-1″), 101.2 (C-1‴), 78.68 (C-5‴), 78.61 (C-5″), 78.55 (C-3‴), 78.54 (C-3″), 74.8 (C-2″), 74.5 (C-2‴), 73.9 (C-8′), 70.9 (C-4″, C-4‴), 66.6 (C-9′), 62.1 (C-6″), 62.0 (C-6‴), 40.2 (C-7′), 34.8 (C-7); ESIMS *m/z* 647.0 $[M+Na]^+$, 668.8 $[M+HCOO]^-$; HRESIMS *m/z* 623.2349 $[M-H]^-$ (calcd for $C_{30}H_{39}O_{14}$, 623.2340).

*4.3.17. Magnoloside V (**17**)*

White amorphous solid; For ^1H NMR (600 MHz, C_5D_5N) and ^{13}C NMR (150 MHz, C_5D_5N) spectroscopic data, see Table 6; ESIMS *m/z* 841.0 $[M+Na]^+$, 816.7 $[M-H]^-$; HRESIMS *m/z* 817.2749 $[M-H]^-$ (calcd for $C_{36}H_{49}O_{21}$, 817.2766).

*4.3.18. Magnoloside W (**18**)*

White amorphous solid; $[\alpha]_D^{20}$ −20.8 (*c* 0.10, MeOH); UV (H_2O) λ_{max} (log ε) 256 (4.48), 293 (4.18) nm; IR (KBr) ν_{max} 3424, 2932, 1706, 1630, 1601, 1510, 1115 cm^{-1}; For ^1H NMR (600 MHz, C_5D_5N) and ^{13}C NMR (150 MHz, C_5D_5N) spectroscopic data, see Table 6; ESIMS *m/z* 811.0 $[M+Na]^+$, 786.7 $[M-H]^-$. HRESIMS *m/z* 787.2666 $[M-H]^-$ (calcd for $C_{35}H_{47}O_{20}$, 787.2661).

*4.3.19. Magnoloside X (**19**)*

Pale yellow amorphous solid; $[\alpha]_D^{20}$ −86.7 (*c* 0.15, MeOH); UV (H_2O) λ_{max} (log ε) 266 (3.88) nm; IR (KBr) ν_{max} 3420, 2935, 1699, 1594, 1508, 1339, 1225, 1131, 968 cm^{-1}; For ^1H NMR (600 MHz, D_2O) and ^{13}C NMR (150 MHz, D_2O) spectroscopic data, see Table 6; ESIMS *m/z* 674.2 $[M+NH_4]^+$; HRESIMS *m/z* 701.2317 $[M+HCOO]^-$ (calcd for $C_{31}H_{41}O_{18}$, 701.2293).

*4.3.20. Magnoloside Y (**20**)*

Pale yellow amorphous solid; For ^1H NMR (600 MHz, C_5D_5N) and ^{13}C NMR (150 MHz, C_5D_5N) spectroscopic data see Table 6; ESIMS *m/z* 665.0 $[M+Na]^+$; HRESIMS *m/z* 641.2088 $[M-H]^-$ (calcd for $C_{29}H_{37}O_{16}$, 641.2082).

*4.3.21. Magnoloside Z (**21**)*

Pale yellow amorphous solid; $[\alpha]_D^{20}$ −89.0 (*c* 0.15, MeOH); UV (H_2O) λ_{max} (log ε) 256 (4.08), 295 (3.78) nm; IR (KBr) ν_{max} 3420, 2933, 1699, 1602, 1273 cm^{-1}; For ^1H NMR (600 MHz, D_2O) and ^{13}C NMR (150 MHz, D_2O) spectroscopic data, see Table 6; ESIMS *m/z* 644.2 $[M+NH_4]^+$; HRESIMS *m/z* 671.2215 $[M+HCOO]^-$ (calcd for $C_{30}H_{39}O_{17}$, 671.2187).

4.4. Sugar analysis of compounds

Compounds **1**–**2**, **6**–**7**, **9**–**11**, **18**–**19**, and **21** (each 2.0 mg) were individually hydrolyzed with 10 mM NaOH (1 mL) at 60 °C for 2 h. Each solution was neutralized and extracted with EtOAc (3 × 1 mL). 2 M CF_3CO_2H (2 mL) was added to the aqueous layer and heated at 110 °C for 3 h. Compounds **12**–**16** (each 2.0 mg) were hydrolyzed with 2 M CF_3CO_2H (2 mL) under the same conditions. After cooling to room temperature, each solution was extracted with EtOAc (3 × 2 ml). Each aqueous layer was then dried by a stream of N_2. The residue and standard D-glucose, D-allose, D-apiose and L-rhamnose were individually dissolved in anhydrous pyridine (100 μL), and L-cysteine methyl ester hydrochloride (0.06 mol/L, 100 μL) was added. The mixture was stirred at 60 °C for 1 h, then 150 μL of HMDS-TMCS (hexamethyldisilazane-trimethylchlorosilane 1:1) was added, and the mixture was stirred at 60 °C for 30 min. The precipitate was removed by centrifugation (10,000 rpm, 10 min), and the supernatant was analyzed by GC using an HP-5 column (30 m × 0.32 mm, 0.25 μm). Temperatures of the injector and detector were both at 250 °C. The temperature of the oven was 230 °C for 30 min (David et al., 2014). Derivatives of L-rhamnose (9.147 min), D-glucose (13.088 min), D-apiose (7.522 min), and D-allose (13.752 min) were detected from those compounds, separately.

4.5. α-Glucosidase inhibitory activity assay

α-Glucosidase (from *Saccharomyces cerevisiae*; Sigma-Aldrich, St. Louis, MO, USA) inhibitory activities were determined by using *p*-nitrophenyl-α-D-glucopyranoside (PNPG) as substrate and acarbose as the positive control, according to the reported method (Liu et al., 2014) with minor modifications. Enzyme solution [50 μL, 0.26 U/mL in 0.05 M potassium phosphate buffer (pH 6.8)] and test compound [50 μL, 1 mM in 0.05 M potassium phosphate buffer (pH 6.8)] were mixed and pre-incubated in 96-well plates for 10 min at 37 °C prior to initiation of the reaction by adding the substrate. After pre-incubation, PNPG solution (100 μL, 5.0 mM in 0.05 M potassium phosphate buffer, pH 6.8) was added and then incubated together at 37 °C for 20 min. After incubation, 0.2 M Na_2CO_3 (100 μL, in 0.05 M potassium phosphate buffer) was added to each well to stop the reaction. The amount of PNP released was quantified by using a Varioskan Flash Multimode Reader (Thermo scientific, Finland) at 405 nm. The percent inhibition of α-glucosidase was calculated as inhibition rate (%) = $[1-(A_{sample}-A_{s\text{-}blank})/(A_{control}-A_{blank})]\times 100$. Samples possessed strong activity, which had an inhibitory rate more than 50% at 1 mM, were further evaluated to obtain their IC_{50} values.

4.6. Cytotoxicity assay

The cytotoxic activity was determined against MGC-803, HepG2, PC3, PC12, MCF-7, A549 and Vero obtained from China center for type culture collection (CCTCC). Measurements were based on a previously reported method (Monks et al., 1991). Cells were seeded in 96-well plates at a cell density of 2–5 × 10^3 per well, 24 h later, treated with various concentrations of compounds. After 72 h of incubation, MTT was added to each well. Then the plates were incubated for 4 h, and the cells were lysed with 150 μL DMSO after removal of the supernatant liquid. Cell viability was measured by observing absorbance at 570 nm on a Varioskan Flash Multimode Reader.

Acknowledgements

The research was financially supported by an 863 Project (2014AA022201).

Appendix A. Supplementary data

Supplementary data associated with this article can be found, in the online version, at http://dx.doi.org/10.1016/j.phytochem.2016.03.011.

References

Argyropoulou, A., Samara, P., Tsitsilonis, O., Skaltsa, H., 2012. Polar constituents of *Marrubium thessalum* Boiss. & Heldr. (Lamiaceae) and their cytotoxic/cytostatic activity. Phytother. Res. 26, 1800–1806.

Chen, J., Wang, B.C., 2005. Advances in pharmacological studies of *Magnoliae officinalis*. J. Chongqing Univ. (natural science edition) 9, 140–143.

David, P., Sibel, A., Anne-Claire, M.O., Tomofumi, M., Chiaki, T., Thomas, P., Stéphanie, D., Patrick, D., Marie-Aleth, L.D., 2014. Triterpenoid saponins from the roots of two *Gypsophila* species. Phytochemistry 102, 182–188.

Deng, S.M., Zhou, J., Cheng, Y.X., Dai, H.F., Tan, N.H., 2000. Two new phenolic glycosides from *Magnolia rostrata*. Chin. Chem. Lett. 11, 1001–1002.

Deng, S.M., Dai, H.F., Zhou, J., 2002. A new glycoside from *Magnolia rostrata*. Acta Bot. Yunnanica. 24, 397–400.

Guo, Z.F., Wang, X.B., Luo, J.G., Luo, J., Wang, J.S., Kong, L.Y., 2011. A novel aporphine alkaloid from *Magnolia officinalis*. Fitoterapia 82, 637–641.

Guo, Z.Y., Li, P., Huang, W., Wang, J.J., Liu, Y.J., Liu, B., Wang, Y.L., Wu, S.B., Kennelly, E.J., Long, C.L., 2014. Antioxidant and anti-inflammatory caffeoyl phenylpropanoid and secoiridoid glycosides from *Jasminum nervosum* stems, a Chinese folk medicine. Phytochemistry 106, 124–133.

Harput, U.S., Genc, Y., Saracoglu, I., 2012. Cytotoxic and antioxidative activities of *Plantago lagopus* L. and characterization of its bioactive compounds. Food Chem. Toxicol. 50, 1554–1559.

Hasegawa, T., Fukuyama, Y., Yamada, T., Nakagawa, K., 1988a. Isolation and structure of magnoloside A, a new phenylpropanoid glycoside from *Magnolia obovate* Thunb. Chem. Lett. 17, 163–166.

Hasegawa, T., Fukuyama, Y., Yamada, T., Nakagawa, K., 1988b. Structures of magnoloside B and C, novel phenylpropanoid glycosides with allopyranose as core the sugar unit. Chem. Pharm. Bull. 36, 1245–1248.

Hwang, Y.P., Kim, H.G., Choi, J.H., Park, B.H., Jeong, M.H., Jeong, T.C., Jeong, H.G., 2011. Acteoside inhibits PMA-induced matrix metalloproteinase-9 expression *via* CaMK/ERK- and JNK/NF-kB-dependent signaling. Mol. Nutr. Food Res. 55, 103–116.

Iwasaki, H., Zhou, Y.Y., 2013. JP Patent 2013035795.

Jabeen, B., Riaz, N., Saleem, M., Naveed, M.A., Ashraf, M., Alam, U., Rafiq, H.M., Tareen, R.B., Jabbar, A., 2013. Isolation of natural compounds from *Phlomis*

stewartii showing α-glucosidase inhibitory activity. Phytochemistry 96, 443–448.
Jiangsu New Medical College, 1977. Chinese Drug Dictionary. Shanghai People Publishing House, Shanghai, pp. 1628–1630.
Liu, Q., 2009. The protective effect and mechanism of *magnolia officinalis* extract on experimental type 2 diabetes in rats Doctoral thesis. Jilin University.
Liu, Q., Hu, H.J., Li, P.F., Yang, Y.B., Wu, L.H., Chou, G.X., Wang, Z.T., 2014. Diterpenoids and phenylethanoid glycosides from the roots of *Clerodendrum bungei* and their inhibitory effects against angiotensin converting enzyme and α-glucosidase. Phytochemistry 103, 196–202.
Miyase, T., Ueno, A., Takizawa, N., Kobayashi, H., Oguchi, H., 1989. Ionone and lignan glycosides from *Epimedium diphyllum*. Phytochemistry 28, 3483–3485.
Monks, A., Scudiero, D., Skehan, P., Shoemaker, R., Paull, K., Vistica, D., Hose, C., Langley, P., Vaigro-Wolff, A., 1991. Molecular targets in the National Cancer Institute drug screen. J. Natl Cancer Inst. 83, 757–766.
Nan, Z.D., Zeng, K.W., Shi, S.P., Zhao, M.B., Jiang, Y., Tu, P.F., 2013. Phenylethanoid glycosides with anti-inflammatory activities from the stems of *Cistanche deserticola* cultured in Tarim desert. Fitoterapia 89, 167–174.
Porter, E.A., Kite, G.C., Veitch, N.C., Geoghegan, I.A., Larsson, S., Simmonds, M.S.J., 2015. Phenylethanoid glycosides in tepals of *Magnolia salicifolia* and their occurrence in flowers of Magnoliaceae. Phytochemistry 117, 185–193.
Sarker, S.D., Latif, Z., Stewart, M., Nabar, L., 2002. Phytochemistry of the genus *Magnolia*. In: Sarker, S.D., Maruyama, Y. (Eds.), The genus *Magnolia*. CRC Press, pp. 32–85.
Shen, C.C., Ni, C.L., Shen, Y.C., Huang, Y.L., Kuo, C.H., Wu, T.S., Chen, C.C., 2009. Phenolic constituents from the stem bark of *Magnolia officinalis*. J. Nat. Prod. 72, 168–171.
Syu, W.J., Shen, C.C., Lu, J.J., 2004. Antimicrobial and cytotoxic activities of neolignans from *Magnolia officinalis*. Chem. Biodivers. 1, 530–537.
Tewari, N., Tiwari, V.K., Mishra, R.C., Tripathi, R.P., Srivastava, A.K., Ahmad, R., Srivastava, R., Srivastava, B.S., 2003. Synthesis and bioevaluation glycosyl ureas as alpha-glucosidase inhibitors and their effect on mycobacterium. Bioorg. Med. Chem. 11, 2911–2922.
Toshio, M., Akira, U., Nobuo, T., Hiromi, K., Hiroko, O., 1988. Studies on the glycosides of *Epimedium grandiflorum* Morr. var. *thunbergianum* (Miq.) nakai. III. Chem. Pharm. Bull. 36, 2475–2484.
Tripetch, K., Ryoji, K., Kazuo, Y., 2002. Phenolic glycosides from *Barnettia kerrii*. Phytochemistry 59, 565–570.
Yan, R.Y., Liu, H.L., Zhang, J.Y., Yang, B., 2014. Phenolic glycosides and other constituents from the bark of *Magnolia officinalis*. J. Asian Nat. Prod. Res. 16 (4), 400–405.
Yang, J.H., Kondratyuk, T.P., Jermihov, K.C., Marler, L.E., Qiu, X., Choi, Y., Cao, H.M., Yu, R., Sturdy, M., Huang, R., Liu, Y., Wang, L.Q., Mesecar, A.D., Breemen, R.B., Pezzuto, J.M., Fong, H.H.S., Chen, Y.G., Zhang, H.J., 2011. Bioactive compounds from the Fern *Lepisorus contortus*. J. Nat. Prod. 74, 129–136.
Ying, Y.M., Zhang, L.Y., Zhang, X., Bai, H.B., Liang, D.E., Ma, L.F., Shan, W.G., Zhan, Z.J., 2014. Terpenoids with alpha-glucosidase inhibitory activity from the submerged culture of *Inonotus obliquus*. Phytochemistry 108, 171–176.
Youn, U.J., Chen, Q.C., Jin, W.Y., Lee, I.S., Kim, H.J., Lee, J.P., Chang, M.J., Min, B.S., Bae, K.H., 2007. Cytotoxic lignans from the stem bark of *Magnolia officinalis*. J. Nat. Prod. 70, 1687–1689.
Yu, S.X., Zhang, C.X., Chen, C.Y., Yan, R.Y., Yang, B., Liao, C.L., You, J.W., 2010. Effects of primary processing on quality of cortex *Magnolia officinalis*. Chin. J Chin. Mater. Med. 35, 1831–1835.
Yu, S.X., Yan, R.Y., Liang, R.X., Wang, W., Yang, B., 2012. Bioactive polar compounds from stem bark of *Magnolia officinalis*. Fitoterapia 83, 356–361.